Best Practice: Generalized k-ω Two-Equation Turbulence Model in ANSYS CFD (GEKO)

Version 1.00

F.R. Menter
R. Lechner
ANSYS German GmbH
A. Matyushenko
NTS, St. Petersburg

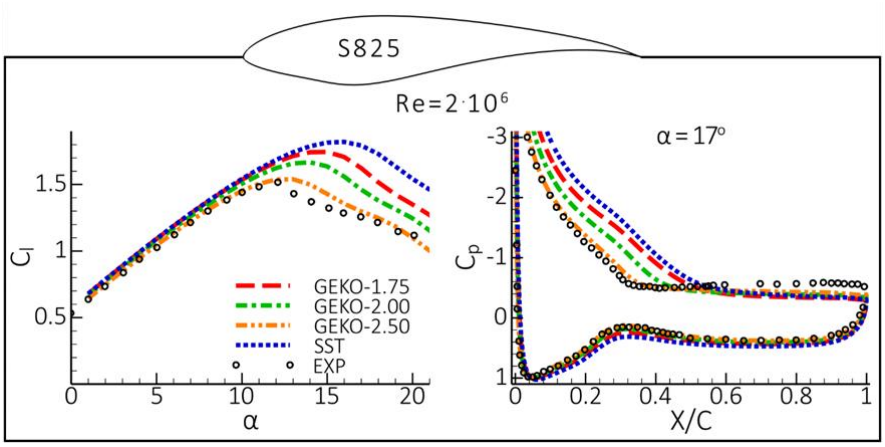

Jan. 2019 Technical Report ANSYS

Table of Contents

1 Motivation

Two-equation turbulence models have matured to a point where a consolidation seems desirable. The main models used in industrial CFD codes today are k-ε [14] (standard and realizable/RKE), k-ω [18,33,34] (SST, BSL, Wilcox) and to a lesser degree V2f [12] (different versions). The differences between the models are not fundamental, but can nevertheless have a strong impact on results. For boundary layers, the models differ mostly in their 'aggressiveness' to predict separation onset. Furthermore, in the very near wall region, models can predict vastly different results, especially for heat transfer simulations, due to their differences in wall-treatment. There are also noticeable differences for free shear flows, where each model tends to favor certain flows over others. Finally, different models feature different limiters, which typically do not affect the baseline flows, but can have substantial influence in complex applications.

ANSYS developed a new turbulence model family called Generalize k-ω (GEKO) model with the goal of turbulence model consolidation. GEKO is a two-equation model, based on the k-ω model formulation, but with the flexibility to tune the model over a wide range of flow scenarios. The key to such a strategy is the provision of free parameters which the user can adjust for specific types of applications without negative impact on the basic calibration of the model. In other words, instead of providing users flexibility through a multitude of different models, the current approach aims at providing one framework, using different coefficients to cover different application sectors. This will substantially simplify code usage for industrial CFD users. This approach also offers a much wider range of calibration capabilities than currently covered by switching between existing models. Finally, GEKO is (or will be made) compatible with all other options in the codes, so that there is no need to select any other model for compatibility or accuracy reasons.

Historically, the coefficients of turbulence models are exposed in the GUI to users (e.g. $C_{\varepsilon 1}$, $C_{\varepsilon 2}$, etc. in a k-ε model). However, this exposure is of little value, as most coefficients are linked to the basic calibration of the model (namely the calibration for the logarithmic law affecting e.g. flat plate simulations). Users can therefore not freely change these values without affecting such flows. In the GEKO model, free coefficients are introduced, which do not affect the logarithmic layer calibration and can therefore by tuned to achieve the desired model behavior. The GEKO model offers six free parameters – two of them aiming at wall bounded flows, two for the calibration of free shear flows, one coefficient to improve corner flow simulations (corner separation) and finally a curvature correction term.

The generic idea behind the model will be discussed. Not all details can be provided as the model is at present unpublished. However, the variability of the model will be demonstrated for a variety of generic flows and Best Practice Guidelines for optimal usage will be provided.

In order to keep the document compact, only a sketch of the geometry is provided for the test cases as well as a the reference to the publication. This is sufficient, as the test cases are typically simple and it is only required to understand the basic flow challenge.

2 The Generalized *k-ω* (GEKO) Model Formulation

2.1 Basic Formulation

The main characteristics of the GEKO model is that it has several free parameters for tuning the model to different flow scenarios. The starting point for the formulation is:

$$\frac{\partial(\rho k)}{\partial t}+\frac{\partial\left(\rho U_j k\right)}{\partial x_j}=P_k-C_\mu\rho k\omega+\frac{\partial}{\partial x_j}\left[\left(\mu+\frac{\mu_t}{\sigma_k}\right)\frac{\partial k}{\partial x_j}\right] \tag{2.1}$$

$$\frac{\partial(\rho\omega)}{\partial t}+\frac{\partial\left(\rho U_j \omega\right)}{\partial x_j}=C_{\omega1}F_1\frac{\omega}{k}P_k-C_{\omega2}F_2\rho\omega^2+\rho F_3 CD+\frac{\partial}{\partial x_j}\left[\left(\mu+\frac{\mu_t}{\sigma_\omega}\right)\frac{\partial\omega}{\partial x_j}\right] \tag{2.2}$$

$$\mu_t=\rho\nu_t=\rho\frac{k}{max(\omega,S/C_{Realize})} \tag{2.3}$$

$$P_k=-\tau_{ij}\frac{\partial U_i}{\partial x_j} \tag{2.4}$$

$$\tau_{ij}^{EV}=-\rho\overline{u_i'u_j'}=\mu_t 2S_{ij}-\frac{2}{3}\rho k\delta_{ij} \tag{2.5}$$

$$CD=\frac{2}{\sigma_\omega}\frac{1}{\omega}\frac{\partial k}{\partial x_j}\frac{\partial\omega}{\partial x_j} \tag{2.6}$$

$$\tau_{i,j}=\tau_{ij}^{EV}-C_{CORNER}\frac{1.2\mu_t}{max\left(0.3\omega,\sqrt{0.5(S^2+\Omega^2)}\right)}\left(S_{ik}\Omega_{kj}-\Omega_{ik}S_{kj}\right) \tag{2.7}$$

with

$$S_{ij}=\frac{1}{2}\left(\frac{\partial U_i}{\partial x_j}+\frac{\partial U_j}{\partial x_j}\right)\quad \Omega_{ij}=\frac{1}{2}\left(\frac{\partial U_i}{\partial x_j}-\frac{\partial U_j}{\partial x_{ji}}\right)$$

$$S=\sqrt{2S_{ij}S_{ij}}\ ;\ \Omega=\sqrt{2\Omega_{ij}\Omega_{ij}}$$

The free coefficients of the GEKO model are implemented through the functions (F_1,F_2,F_3) which can be tuned by the user to achieve different goals in different parts of the simulation domain. Currently there are six parameters included for that purpose:

- C_{SEP}
  - Main parameter for adjusting separation prediction for boundary layers
  - Affects all flows - Increasing C_{SEP} reduces eddy-viscosity leading to more sensitivity to adverse pressure gradients for boundary layers and to lower spreading rates for free shear flows (compensated by C_{MIX})
- C_{NW}
  - Affects mostly the inner part of wall boundary layers (limited to no impact on free shear flows.
  - Increasing C_{NW} leads to higher wall shear stress and wall heat transfer rates in non-equilibrium flows.

  - Effect on non-generic flows (e.g. vortices) moderate but not systematically tested
  - Users can mostly use C_{NW} = 0.5 (default)
- C_{MIX}
  - Affects only free shear flows (boundary layer shielded due to function F_{blend}).
  - Increasing C_{MIX} increases spreading rates of free shear flows
  - For each value of C_{SEP} an optimal value of C_{MIX} exists, which maintains optimal free shear flows. This value is given by the correlation $C_{MIX}=C_{MixCor}$ which is default

$$C_{MixCor} = 0.35\text{sign}\left(C_{Sep} - 1\right)\sqrt{\left(\left|C_{Sep} - 1\right|\right)}$$

- C_{JET}
  - Is active in a sub-model of C_{MIX} (no impact for C_{MIX} = 0).
  - Affects mostly jet flows. Increasing C_{JET} while C_{MIX} is active, decreases spreading rate for jets.
  - Allows to adjust spreading rate of jet flows while maintaining spreading rate of mixing layer.
  - Users can mostly use C_{JET} = 0.9 (default)
  - Has no effect in case of C_{MIX} = 0
- C_{CORNER}
  - Non-linear stress-strain term to account for secondary flows in corners (e.g. wing-body junctions etc. [17]).
- C_{CURV}
  - An existing model for curvature correction, which can be combined with the GEKO model [27,19]

All coefficients (except of C_{JET} which is of minor importance) can be accessed globally or locally through User Defined Functions (UDFs), allowing a global or zonal model optimization.

The coefficients C_{SEP} and C_{NW} affect boundary layers, whereas C_{MIX} and C_{JET} are designed for free shear flows. In order to avoid any influence of C_{MIX} and C_{JET} onto boundary layers, a blending function is introduced, which de-activates C_{MIX} and C_{JET} in the boundary layer. The function is similar to the blending function used in the BSL/SST model formulation and given by:

$$\begin{aligned} L_T &= \frac{\sqrt{\tilde{k}}}{C_\mu \omega} \\ \tilde{k} &= max(k, CFb_{Lam} \cdot \omega) \\ x_{blend} &= CFb_{Turb}\frac{L_T}{y} \\ F_{GEKO} &= tanh({x_{blend}}^4) \end{aligned} \tag{2.8}$$

This function activates the free shear flow parameters as follows:

$$F_{Free} = C_{MIX} F_{Jet}(C_{JET})(1 - F_{Blend}) \tag{2.9}$$

There are two important aspects. Firstly, the function $F_{Blend} = 1$ inside boundary layers and $F_{Blend} = 0$ for free shear flows. Secondly, the parameter C_{JET} is a sub-parameter of C_{MIX}. It only affects the simulation in case $C_{MIX} \neq 0$.

The free coefficients should be in the range (defaults in parenthesis):

MIN		Parameter	MAX			Default
0.7	≤	C_{SEP}	≤	2.5		1.75
-2.0	≤	C_{NW}	≤	2.0		0.50
... 0.5	≤	C_{MIX}	≤	1.0…		C_{MixCor}
0.0	≤	C_{JET}	≤	1.0		0.90
0.0	≤	C_{CORNER}	≤	1.5		1.00
0.0	≤	C_{CURV}	≤	1.5		1.00

(2.10)

The greyed values for C_{MIX} are only suggestions. There might be situations where values lower than 0.5 or higher than 1.0 can be appropriate.

As mentioned above, for the coefficient C_{MIX} a correlation is provided as default, which ensures that changes in C_{SEP} do not negatively affect free mixing layers:

$$C_{MixCor} = 0.35\text{sign}(C_{Sep} - 1)\sqrt{(|C_{Sep} - 1|)} \tag{2.11}$$

2.2 Limiters and Realizability

It is well-known that any conventional two-equation model exhibits build-up of turbulence in stagnation regions of bluff bodies (like leading edges of airfoils etc.). The reason lies in the substitution of the eddy-viscosity assumption into the production term P_k of the two-equation model. The eddy-viscosity assumption is not representing the physics correctly in such regions and leads to an over-production of turbulence kinetic energy, which in turn can lead to excessive eddy-viscosity levels in these areas. This can have a detrimental effect on the flow over the rest of the geometry, as the boundary layers starting from the leading edge stagnation point would be predicted incorrectly. This can cause large errors and even false separation. Such situations do not only appear in classical stagnation zones of airfoils, but in many technical flows, where flows hit on a surface or different flow streams collide to form a stagnation region.

There are numerous remedies for that problem. The most widely known is the use of the so-called Kato-Launder correction [15] whereby the square of the shear strain in P_k is replaced by strain times vorticity:

$$P_k = \mu_t S^2 \quad \rightarrow \quad P_k = \mu_t S\Omega \tag{2.12}$$

This option is available, albeit typically not by default. It is however activated when using the GEKO model in combination with a model for laminar-turbulent transition, as it prevents even small production rates which can have a significant effect on transitional flows. It should be noted that the Kato-Launder modification can have an effect on flows with rotation and swirl relative to the original model calibration. It also leads to un-physical production in rotating systems as pointed out by Durbin and Reif [11] and should therefore be applied with caution.

An alternative was proposed by Menter [17] in form of a production limiter:

$$\tilde{P}_k = min\left(P_k, C_{PK\,lim}\rho\varepsilon\right) \tag{2.13}$$

The limiting coefficient can be chosen fairly large (typically $C_{PKlim}=10$), relative to the equilibrium relation $P_k/(\rho\varepsilon)=1$. It will therefore not affect any calibrated flow and still avoids the stagnation build-up and is used as a default option in GEKO (as in all other k-ω based models in ANSYS CFD).

A more theoretical concept can also be applied by imposing a realizability constraint. Realizability demands e.g. that all normal Reynolds Stress components need to always remain positive (e.g. [11]). This is clearly true from a physical standpoint, but can be violated by eddy-viscosity models (as well as EARSM and RSM). One can argue about how important this constraint is from a practical standpoint, as eddy-viscosity models do not attempt to accurately describe each single Reynolds Stress, but model essentially the principal shear stress. Still, the realizability constraint can, as a side-effect, help to avoid stagnation build up. For eddy-viscosity models it reads:

$$\nu_t = min\left(\frac{k}{\omega}, C_{Realize}\frac{k}{S}\right) = \frac{k}{max(\omega, S/C_{Realize})}; \quad C_{Realize} = \frac{1}{\sqrt{3}} \approx 0.577 \tag{2.14}$$

The realizability limiter has the additional benefit to prevent numerical break-down in case ω approaches zero at any point in the domain. Without the constraint in the denominator, this would lead to arbitrarily high eddy-viscosities, whereas with the limiter, such points are typically handled gracefully.

In the GEKO model the realizability limiter is utilized in addition to the production limiter by default. Users can change the values of both coefficients.

2.3 Near Wall Treatment

The near wall formulation of a turbulence model has a substantial effect on its accuracy and its robustness. In addition, modern CFD codes typically feature so-called y+-insensitive wall formulations, which allow the user to obtain sensible simulations over a wide range of grids with different y^+ near wall resolutions.

The GEKO model family was designed by sticking closely to the original *k-ω* model formulation – following the argument that the modeled *k* is proportional to $\overline{v'v'}$ and not to the physical turbulence kinetic energy. The peak observed in the turbulence kinetic energy in the buffer layer is therefore not modelled, as it consists mostly of passive motion (no effect on shear stress).

A y^+-insensitive wall formulation has been developed for the GEKO model (similar to what is used in the BSL and SST models). It allows the use of the model, on meshes of

arbitrary y^+ values, as long as the y^+-value lies in the logarithmic layer of the boundary layer, and as long as the rest of the boundary layer is resolved with a sufficient number of cells.

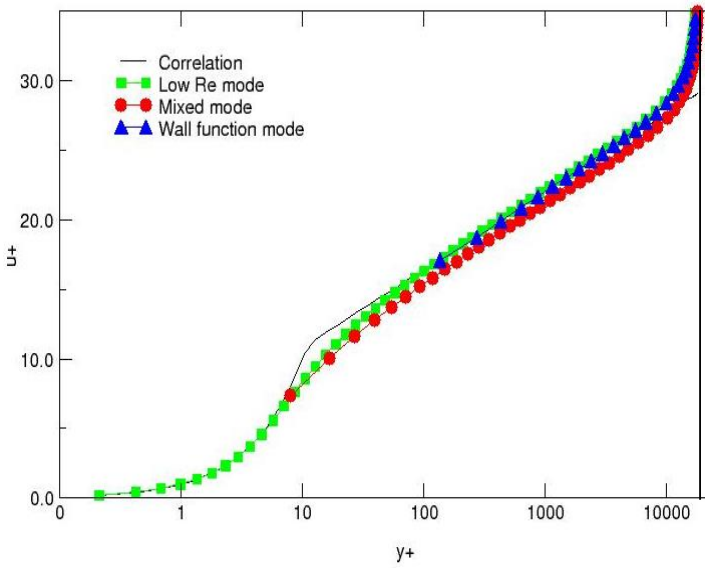

Figure 1: Near wall y+-insensitive wall treatment for GEKO model.

The y^+-insensitive wall formulation has the advantage that users do not have to select a wall treatment. The optimal formulation is selected by the formulation based on the grid provided.

It is important to counter a widely held belief that *k-ω* based models require a finer near wall resolution than say a *k-ε* model with wall functions. This is not correct, as the y^+-insensitive wall formulation blends to the exact same wall function once the grid is coarsened.

In order to demonstrate the superior behavior of k-ω based models compared with other models, a backstep was computed on a y+~1 mesh. The wall shear stress and Stanton number (heat transfer) distribution downstream of the step are shown in Figure 2. All curves are based on the same high Re number k-ε model (the GEKO model is set to an exact transformation of k-ε). The ML is a low Re number k-ε model, EWT is a 2-layer formulation [35] and the V2f model is an extension of k-ε with elliptic blending [12]. While all baseline models are essentially identical, the differences in near wall formulation results in very large differences between the results. It is obvious that the GEKO model is closest to the experimental data.

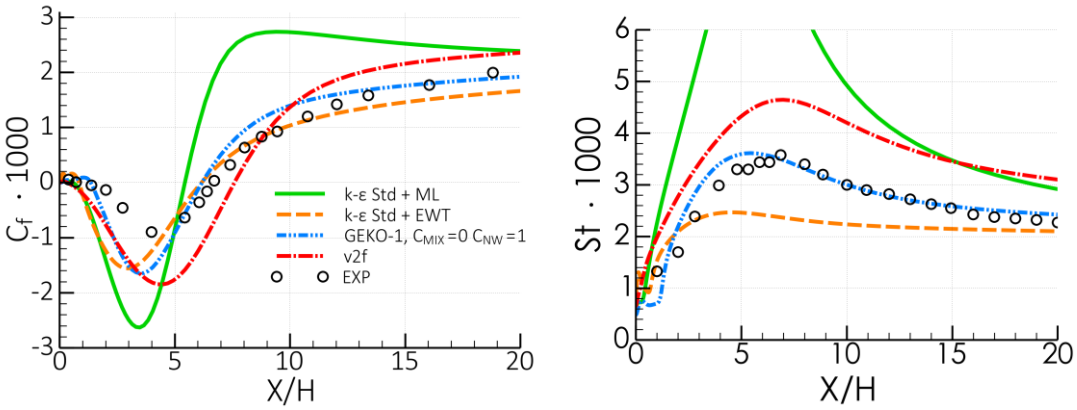

Figure 2: Wall shear stress coefficient, C_f (left) and wall heat transfer coefficient, St, (right) for backward-facing step flow [31]

2.4 Terminology

In order to clearly characterize the model variant used in an application, it is important to have a unified terminology for the model. It is proposed to just name the coefficients which are not default.

- GEKO with C_{SEP}=1.2, C_{NW}=1.0, C_{MIX}=1.0, C_{JET}=0.9 would be termed
  - GEKO:(C_{SEP}=1.2, C_{NW}=1.0, C_{MIX}=1.0).
- GEKO with C_{SEP}=1.5, C_{NW}=0.0, C_{MIX}=C_{MixCor}, C_{JET}=1.0 would be termed
  - GEKO:(C_{SEP}=1.5, C_{NW}=0.0, C_{JET}=1.0).
- Situations where only C_{SEP} is changed (most frequent case) will just be characterized in short notion:
  - GEKO with C_{SEP}=1.5 will be termed GEKO-1.5

3 The Influence of the Free GEKO Parameter

3.1 The 'Separation' Parameter C_{SEP}

The ability to predict separation depends mostly on the level of the eddy-viscosity in the boundary layer. A suitable approach for tuning the model to adverse pressure gradients and separation is to allow a re-calibration of the basic model constants, while at the same time maintaining the calibration for the slope of the logarithmic layer and the proper near wall viscous damping required for achieving the correct shift in the log-layer (and thereby the correct wall shear stress). This is achieved by using the free parameter C_{SEP}.

Figure 3 shows the effect of C_{SEP} on a flat plate boundary layer computation for the ratio $EVR = \mu_t/\mu$. Increasing C_{SEP} from C_{SEP}=1.00 to C_{SEP}=1.75 leads to a significant reduction in the ER levels. (Note that the effect is even more pronounced for flows with adverse pressure gradients and separation).

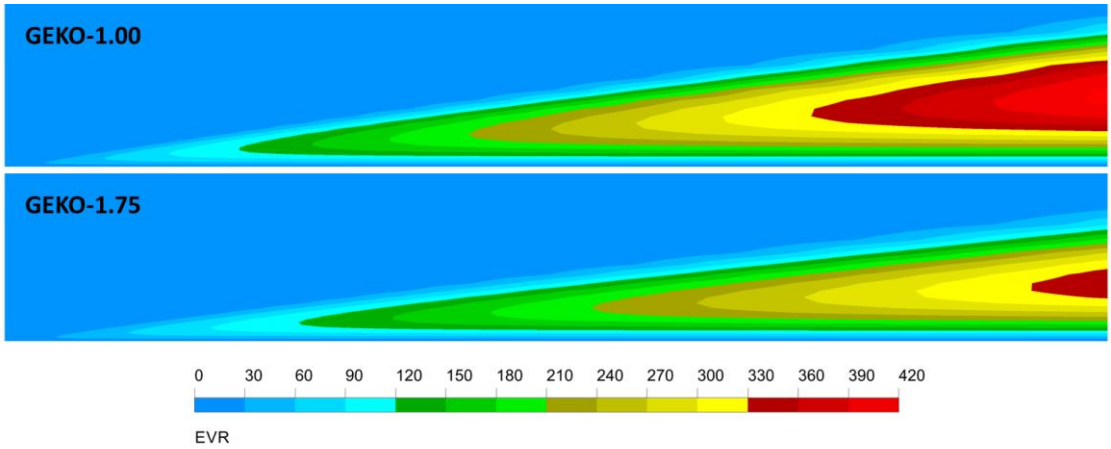

Figure 3: Change of the eddy-viscosity ratio (EVR) under changes of C_{SEP} for a flat plate. Top: C_{SEP}=1.0 (all else default). Bottom C_{SEP}=1.75 (all else default)

Figure 4 shows that even large changes in C_{SEP} do not have any effect on the wall shear stress (C_f) and heat transfer coefficients (St). This is the basic design criterion for the GEKO model. It ensures that the user can adjust coefficients like C_{SEP} freely (within range).

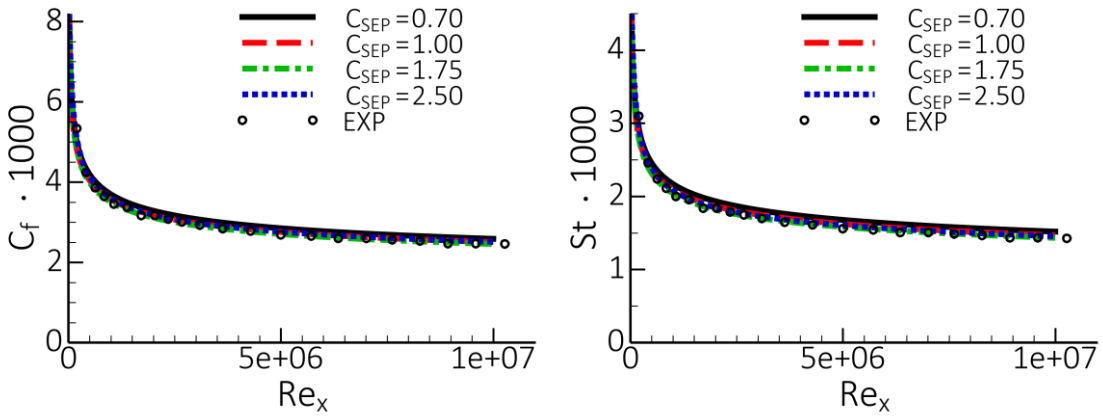

Figure 4: Flat plate boundary layer under variation of C_{SEP} (C_{NW}=0.5). Left : Wall-shear stress coefficient, C_f, Right: Wall heat transfer coefficient, St.

The independence of the mean flow velocity is also illustrated by the logarithmic velocity profiles shown in Figure 5. Again, the logarithmic velocity profile is maintained over a wide range of C_{SEP} coefficients.

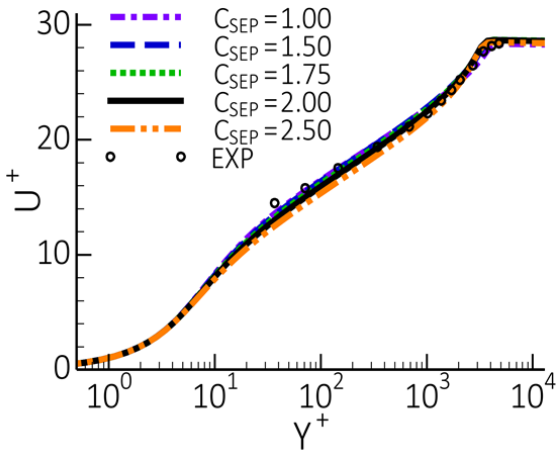

Figure 5: Velocity profiles in logarithmic plot under variation of C_{SEP} for flat plate

The effect of C_{SEP} on an equilibrium adverse pressure-gradient boundary layer flows is demonstrated for the experiment of Skare and Krogstad ($\beta_T=20$, $Re_{\delta*}=1.0x10^5$) [21]. The simulations are based on the equilibrium boundary layer equations as given by Wilcox [31]. The non-dimensional pressure gradient $\beta_T=20$ drives the flow close to separation, a regime, which is very sensitive to turbulence modeling. The left part of Figure 6 shows the influence of C_{SEP} on the velocity profiles whereas the right part shows the impact on the non-dimensional eddy-viscosity, $NUT = \nu_t/(U_\delta \delta^*)$ (U_δ is the velocity at the edge of the boundary layer and δ* is the displacement thickness). The velocity profile exhibits moderately but visibly more decelerated with increasing C_{SEP}. The eddy-viscosity, however, is drastically reduced by more than a factor of two by the variation of C_{SEP} between 1-2. The most accurate solution is the one with C_{SEP}=1.75. This reduction in eddy-viscosity is desirable for adverse pressure-gradient boundary layers, as low values increase the sensitivity of the model to adverse pressure gradients and separation. Note that the coefficients C_{MIX}, C_{JET} have little effect on the boundary layer flows, due to the blending function being mostly equal to one inside the boundary layer. The parameter C_{NW} was set to its default value C_{NW}=0.5 (as will be detailed later). However, variations of C_{NW} would have little effect on the current flow.

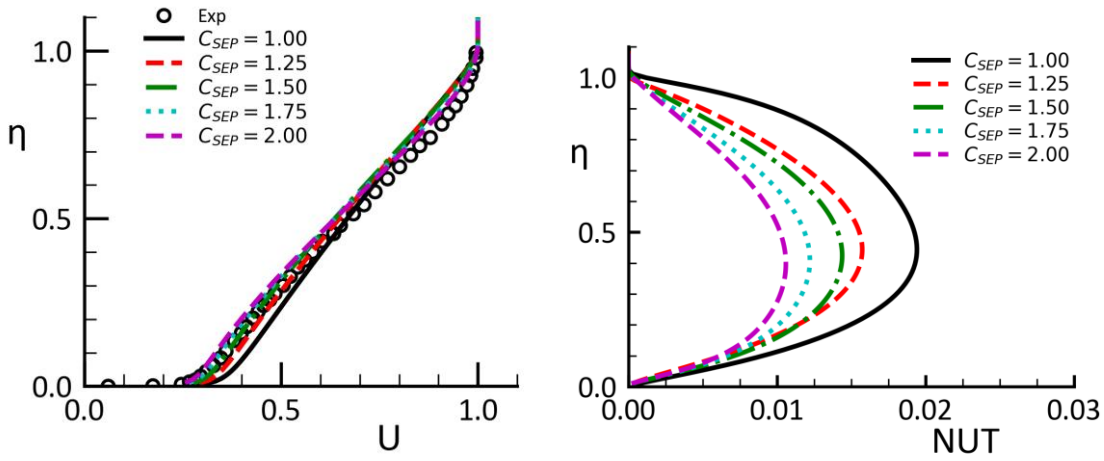

Figure 6: Impact of variation in C_{SEP} on boundary layer with adverse pressure gradient. Left: Velocity profile. Right Eddy-viscosity profiles

The effect of variation in C_{SEP} is shown in Figure 7 for the axi-symmetric diffuser flow of Driver et al [10] (C_{NW}=0.5, C_{MIX}=C_{MixCor}, C_{JET}=0.9). As expected from the results for the equilibrium boundary layer, with increasing C_{SEP}, the model becomes more sensitive to the adverse pressure gradient in the diffuser and improves its separation predict up to a value of C_{SEP}~1.75-2.00. Higher values of C_{SEP} lead to over-separation. Note that an optimal calibration of a turbulence model for the CS0 diffuser, does not necessarily guarantee an optimal solution for other similar flows. As will be shown below, for 2D airfoils more 'aggressive' settings are required to match the exp. data. It is therefore desirable that the GEKO model can be pushed to over-separation for the CS0 case.

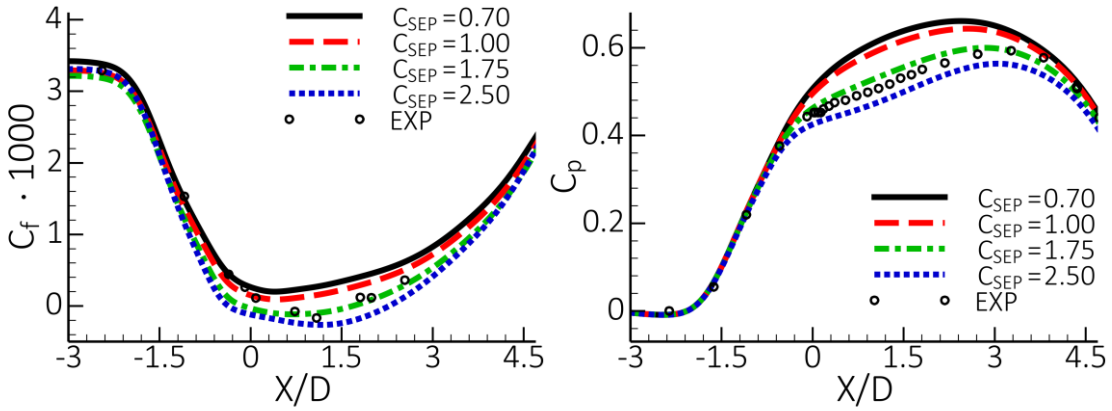

Figure 7: Impact of variation in C_{SEP} on CS0 diffuser flow [10]. Left wall shear stress coefficient, C_f. Right: Wall pressure coefficient C_p

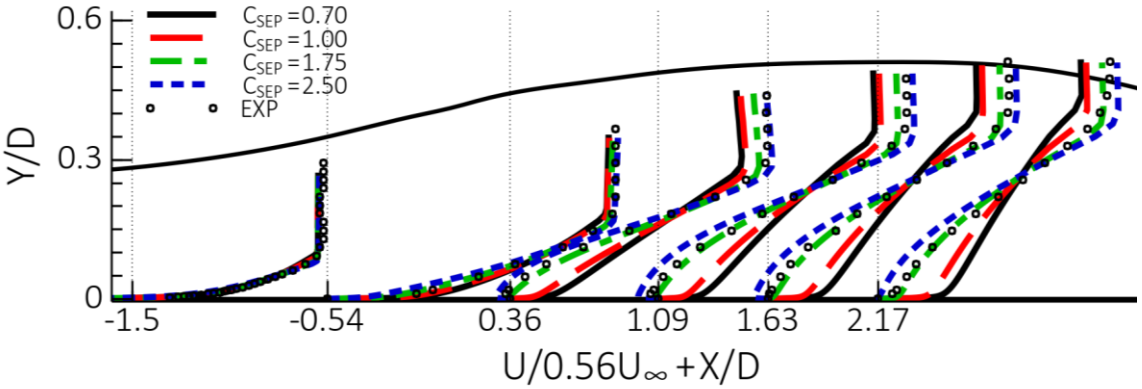

Figure 8: Impact of variation in C_{SEP} on velocity profiles for CS0 diffuser flow [10]

A more realistic application for tuning the C_{SEP} coefficient is the simulation of 2D airfoil profiles under variation of the angle of attack, α. Figure 9 to Figure 13 compare lift curves for numerous airfoils computed with the GEKO model. In these comparisons, it should be kept in mind that 2D simulations are not entirely correct in the stall and post-stall region (around and past maximum lift, C_{Lmax}), due to the formation of 3D structures in the experiments. Despite of this, it is possible to adjust the GEKO model for the prediction of such flows for angles of attack in 2D simulations. Increasing C_{SEP} predicts earlier separation

onset, which improves agreement of the predicted pressure coefficient and results in an improved agreement of the lift coefficient with the experimental data[1] near stall. The optimal value for C_{SEP} for such flows is therefore somewhere between C_{SEP}=2.00-2.50.

The current test cases demonstrate the advantage of the GEKO model over e.g. the SST model. The SST model is tuned to match adverse pressure gradients flows and flows with separation well on average. However, for the 2D airfoils the SST model is clearly too conservative resulting in overly optimistic C_{Lmax} levels. This would be hard to correct within the SST model and in any case would require expert knowledge in turbulence modeling. Within the GEKO model, separation prediction can easily be adjusted by changing C_{SEP} even by a non-expert.

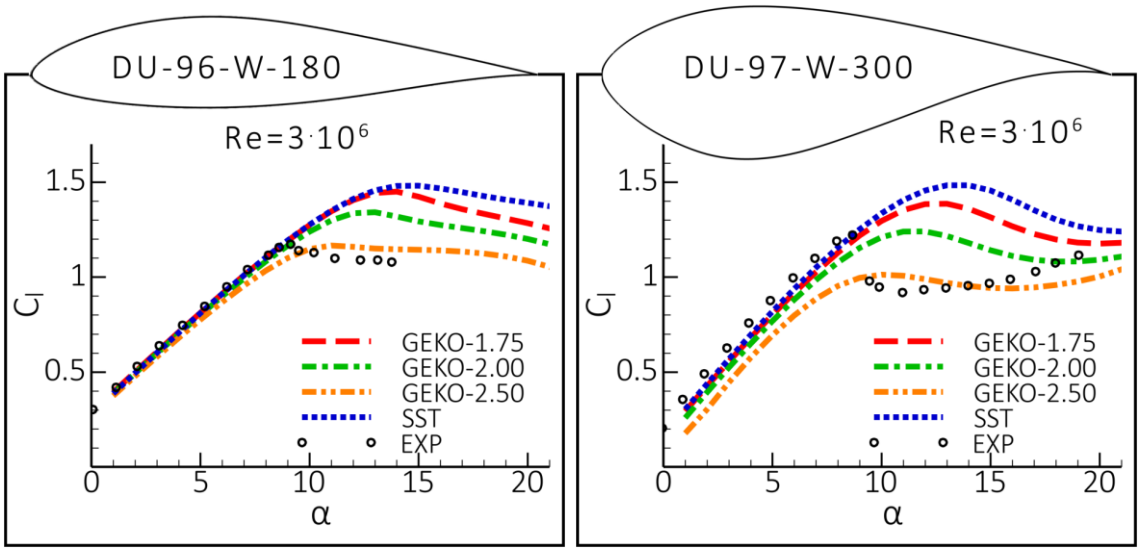

Figure 9: Prediction of lift and pressure coefficients with GEKO model for DU-96-W-180 (Left) and DU-97-W-300 (Right) airfoil at Re=3·10⁶ [28]

[1] There are no experimental data for the pressure coefficients for the DU-96-W-180 and DU-97-W-300 airfoils. Only distribution of lift coefficient in wide range of angles of attack are available.

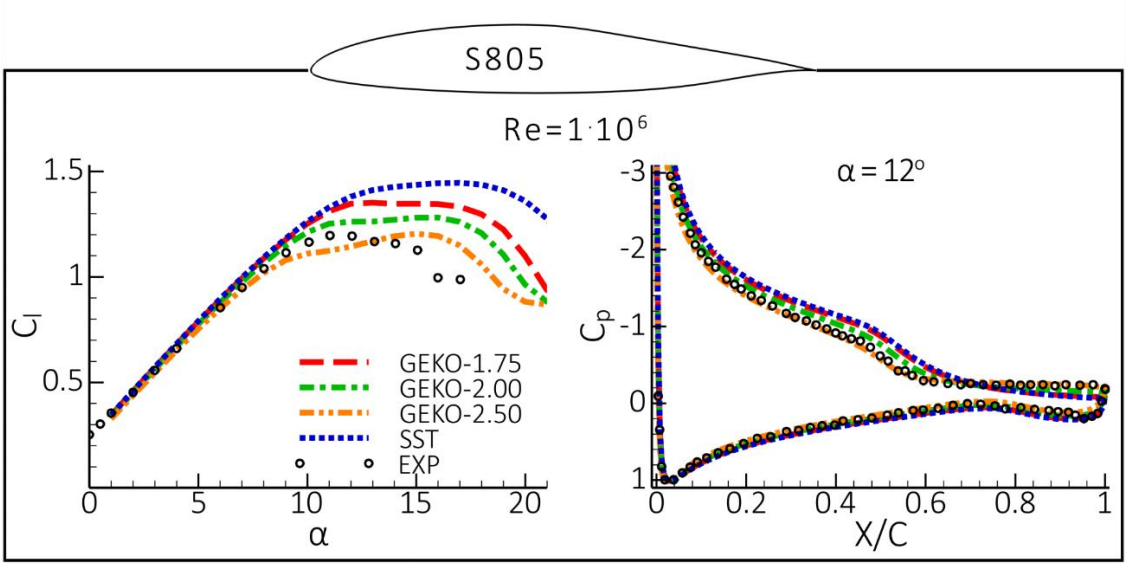

Figure 10: Prediction of lift coefficient in wide range of angle of attacks (Left) and pressure coefficient for α = 12º (Right) with GEKO model for S805 airfoil at Re=1·10^6 [23]

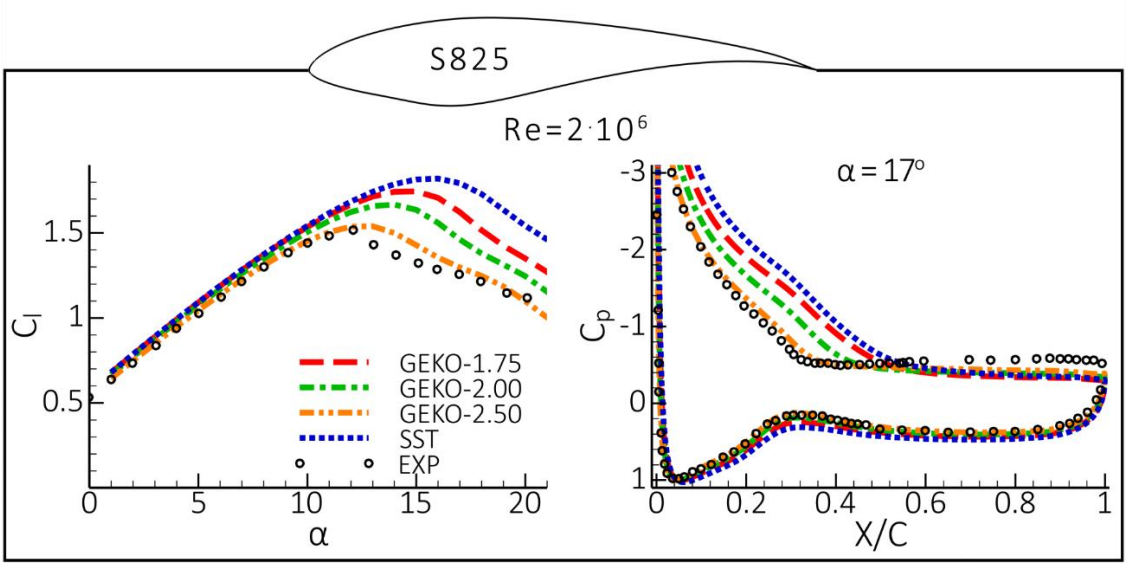

Figure 11: Prediction of lift coefficient in wide range of angle of attacks (Left) and pressure coefficient for α = 17º (Right) with GEKO model for S825 airfoil at Re=2·10^6 [24]

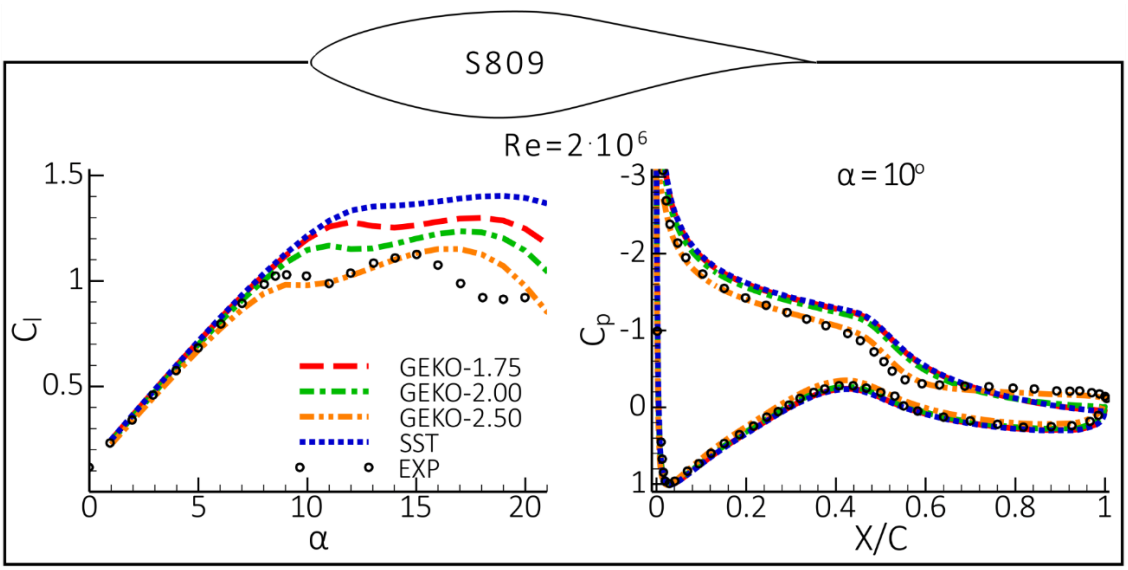

Figure 12: Prediction of lift coefficient in wide range of angle of attacks (Left) and pressure coefficient for α = 10° (Right) with GEKO model for S809 airfoil at Re=2·10⁶ [25]

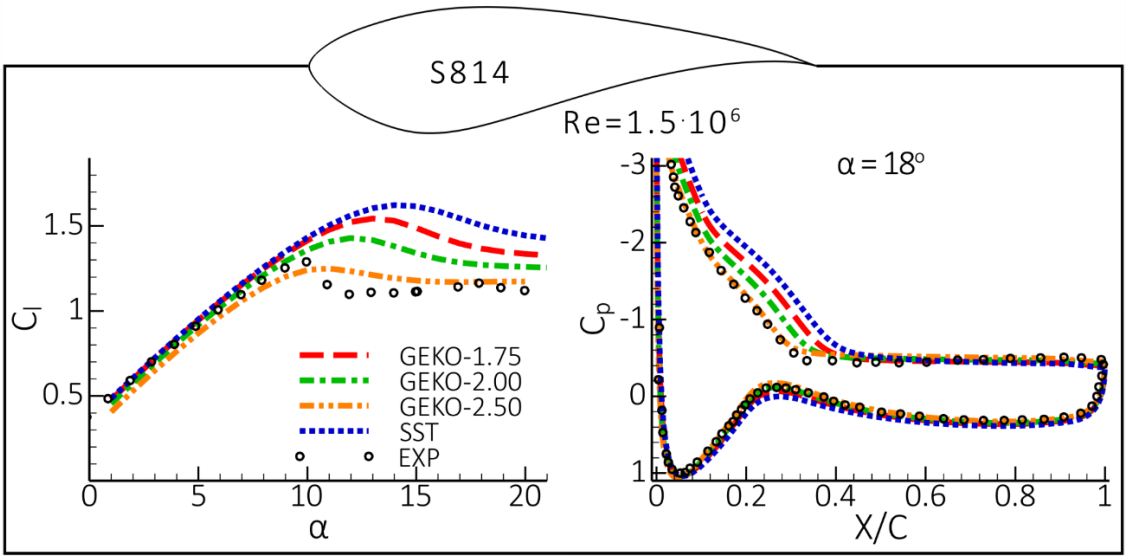

Figure 13: Prediction of lift coefficient in wide range of angle of attacks (Left) and pressure coefficient for α = 18° (Right) with GEKO model for S814 airfoil at Re=1.5·10⁶ [26]

It is important to understand that changes of C_{SEP} affect not only boundary layers, but the entire flow field. Increasing C_{SEP} reduces the eddy-viscosity in all parts of the domain, including for free shear flows (e.g. mixing layers etc.). Frequently, the adjustment of boundary layer separation is the main optimization requirement and it is desirable to maintain the performance and calibration for free shear flows (e.g. spreading rates for mixing layers and jets etc.). In order to avoid any negative impact of C_{SEP} on free shear flows, the reduction in eddy-viscosity is corrected by modifying C_{MIX} accordingly. This is achieved through the correlation C_{MixCor} given in Equation (2.11). This correlation increases C_{MIX} with increasing C_{SEP} to maintain the spreading rates for mixing layers. As the correlation C_{MIX} =C_{MixCor} is default, users do not have to adjust C_{MIX} when changing C_{SEP}. This effect will be demonstrated in the Section 3.3 dealing with the impact of C_{MIX}.

The Bachalo-Johnson NASA Bump flow experiment [2], as depicted in Figure 14, features a subsonic inflow with Ma=0.875. The flow is then accelerated to supersonic speed over the bump and then reverts to subsonic speed through a shock wave. The shock causes the boundary layer behind the shock to separate, which in turn interacts with the shock by pushing it forward. The ability to predict the shock location is therefore directly linked to a model's ability to predict boundary layer separation. As expected, again, the models group as GEKO-1.75/SST and GEKO-1.00/RKE as seen from Figure 15. Both, the GEKO-1.75 and the SST model can predict the shock location and the post-shock separation zone properly. The GEKO-1.00/RKE models fail due to their lack of separation sensitivity.

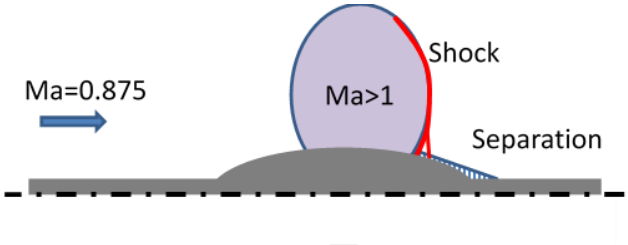

Figure 14: Schematic of transonic axi-symmetric bump flow

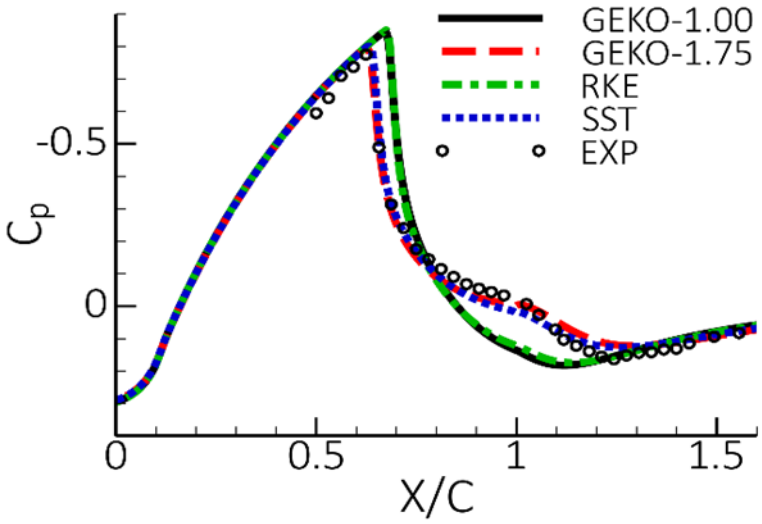

Figure 15: Pressure coefficient, C_p, along wall of bump. Comparison of different GEKO settings with RKE and SST model and experimental data [2].

3.2 The 'Near Wall' Parameter C_{NW}

The coefficient C_{NW} is introduced to allow a modification of the model characteristics in the near wall region under non-equilibrium conditions. It has a strong effect on heat transfer predictions in reattachment and stagnation regions.

The first task is to show that variations in C_{NW} (like C_{SEP}) do not affect flat plate boundary layer behavior. This can be seen from Figure 16 where both, the wall shear stress coefficient, C_f, and the wall heat transfer coefficient St are unaffected by variations in C_{NW}. In addition,

the velocity profile in log-scale is maintained as shown in Figure 17. Many more variations of parameters C_{SEP} and C_{NW} have been tested and the agreement is like that shown in Figure 17.

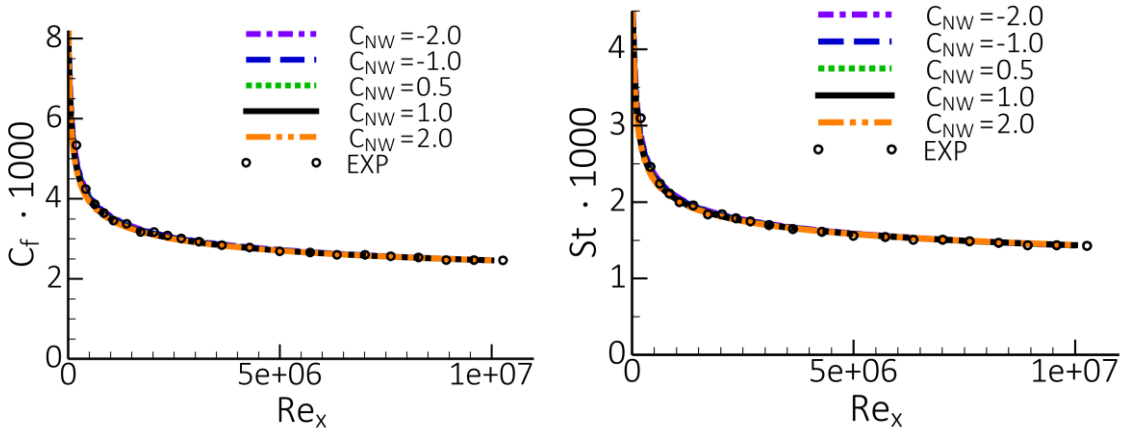

Figure 16: Flat plate boundary layer under variation of C_{NW} (C_{SEP}=1.75). Left : Wall-shear stress coefficient, C_f, Right: Wall heat transfer coefficient, St.

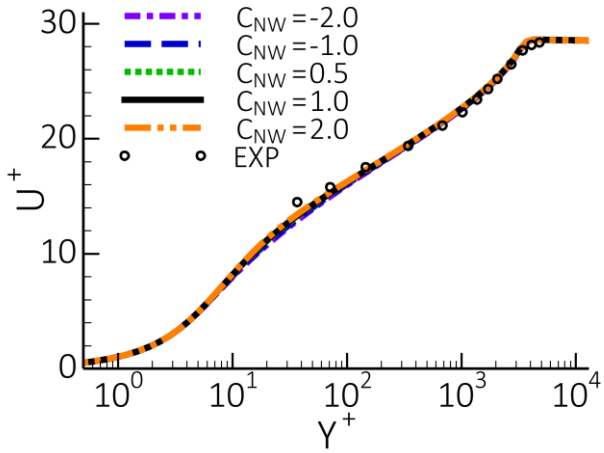

Figure 17: Velocity profiles in logarithmic coordinates - variation of C_{NW} (C_{SEP}=1.75)

The effect of changing C_{NW} for the axisymmetric diffuser test case CS0 [10] is shown in Figure 18. The coefficient C_{NW} is designed to have an influence mostly near the wall. Therefore, the wall shear-stress distribution shows a much larger sensitivity to this variation (Figure 18 Left) than the C_p-distribution (Figure 18 Right). The velocity profiles shown in Figure 19 illustrate the effect more clearly. Contrary to changes of C_{SEP}, where the entire boundary layer is affected, variations in C_{NW} change only the inner part of the velocity profiles.

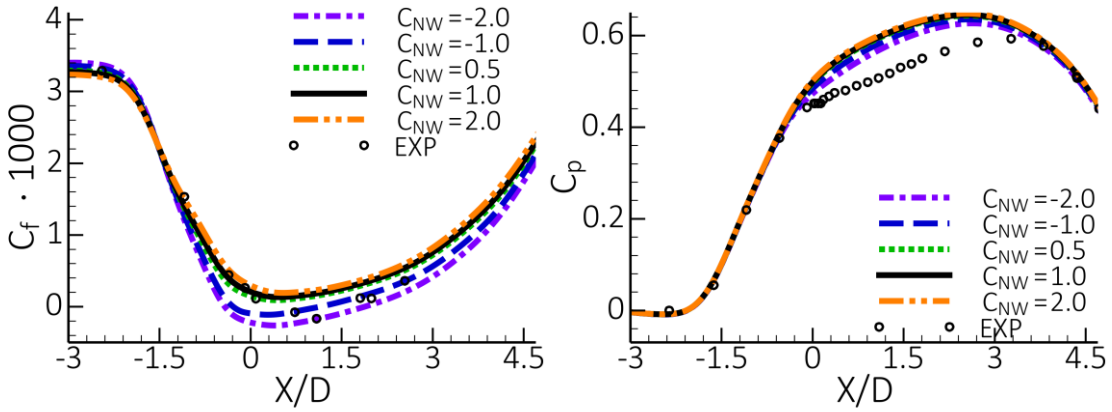

Figure 18: Impact of variation in C_{NW} on CS0 diffuser flow [10]. Left: Wall shear-stress coefficient, C_f. Right: Wall pressure coefficient C_p (C_{SEP}=1.0, C_{MIX}=0.0, C_{JET}=0.9)

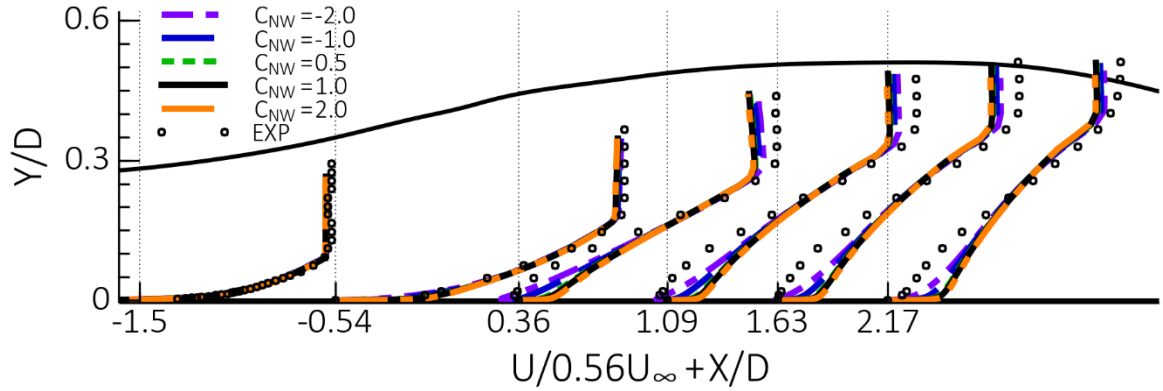

Figure 19: Impact of variation in C_{NW} on velocity profiles for CS0 diffuser flow [10]

For non-equilibrium flows, the wall shear stress and more importantly, the heat transfer to a wall, depend mostly on the model details close to the wall. The coefficient C_{NW} can be tuned to allow fine-tuning for such flows. An example is backward-facing step with C_f and heat transfer measurements, St, downstream of the step [31]. The effect is shown in Figure 20. It is computed with both, C_{SEP}=1.0 and C_{SEP}=1.75, C_{MIX}=C_{MixCor} , C_{JET}=0.9 and a variation in C_{NW}. The heat transfer is strongly affected (and can therefore be optimized) by changes in C_{NW}. In the current application, the optimal value is C_{NW}=0.5 for both values of C_{SEP}. C_{NW}=0.5 is also the default setting. It is important to note that C_{NW} is a minor parameter and will likely not have to be tuned for most flows. Wider validation studies indicate that the default value is suitable for most applications.

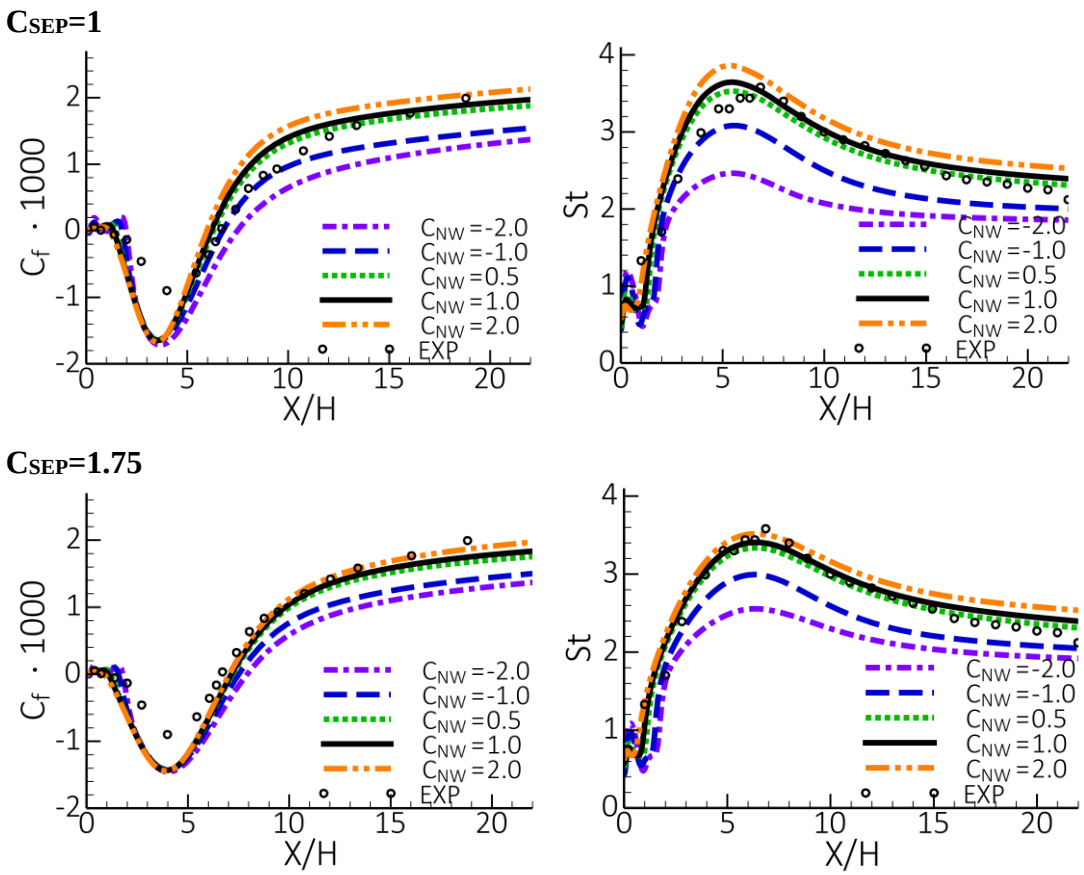

Figure 20: Backward-facing step with heat transfer under variation of C_{NW} (Top: C_{SEP}=1.00, Bottom: C_{SEP}=1.75, Both: C_{JET}=0.9, C_{MIX}=C_{MixCor}). Left: Wall shear stress coefficient, C_f, Right: Heat transfer Stanton number

3.3 The 'Mixing' Parameter C_{MIX}

The parameter C_{MIX} affects only free shear flows. It has no impact on boundary layers due to the blending function F_{Blend}. Increasing C_{MIX} leads to larger eddy-viscosity (higher turbulence levels) in free shear flows. This is illustrated in Figure 21 which shows results for a mixing layer simulation compared with experimental data [3]. As expected, increasing C_{MIX} leads to larger spreading rates of the velocity profile, associated with higher levels of turbulence kinetic energy. In most applications, it is desirable to calibrate the coefficient such that a good agreement with mixing layer flows is achieved (in the current example with C_{SEP}=2 this means C_{MIX}=0.35). However, there can be cases, where stronger mixing is desired and where the calibration for a classical mixing layer is not sufficient. Examples are flows with strong mixing characteristics, like flows past bluff bodies etc. It should be emphasized that the physical reason for increased mixing in such cases is often a result of flow unsteadiness (e.g. vortex shedding) augmenting the conventional turbulence mixing. In such cases it will not be possible to obtain a perfect agreement against data, as such unsteady effects are typically stronger than that which a turbulence model can provide. Still, increasing C_{MIX} can at least compensate for some of the missing effects, in case that unsteady (scale resolving) simulations are not feasible.

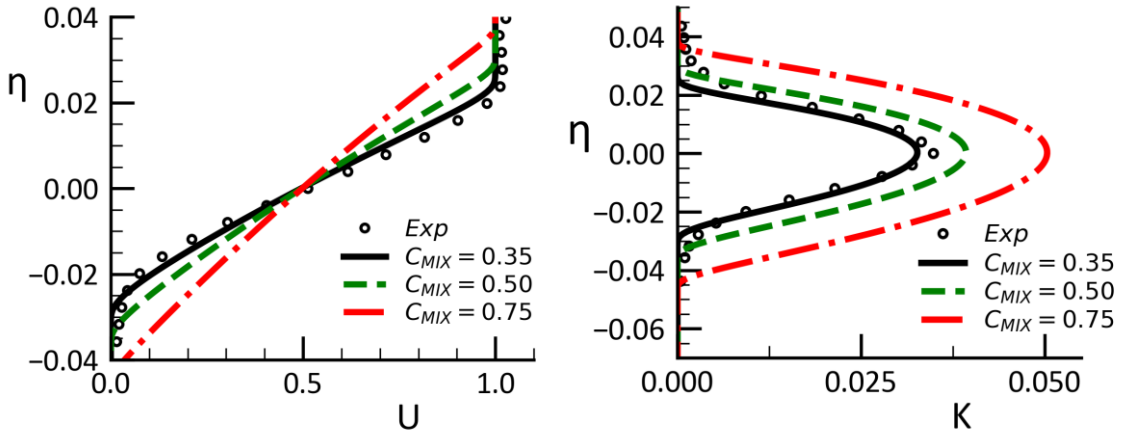

Figure 21: Impact of variation in C_{MIX} on mixing layer when using the C_{SEP}=2 (C_{JET}=0.9, C_{NW}=0.5). Left: Velocity profile. Right: Turbulence kinetic energy profiles

As already mentioned in the section on C_{SEP} (section 3.1), there is a subtle interaction of C_{MIX} and C_{SEP} which users have to understand. Variations in C_{SEP} also affect free shear flows and increases in C_{SEP} result in lower spreading rates. This can be seen in Figure 22 which shows the results of a C_{SEP} variation for the mixing layer [3] (C_{MIX} = 0, C_{JET} = 0.9, C_{NW} = 0.5). Here the solution with C_{SEP} = 1 is closest to the data whereas the solution with C_{SEP}=2 predicts far too low spreading rates and turbulence levels. The effect on the eddy-viscosity is even stronger than for the boundary layer resulting in a reduction of more than a factor 3 with increasing C_{SEP} (not shown).

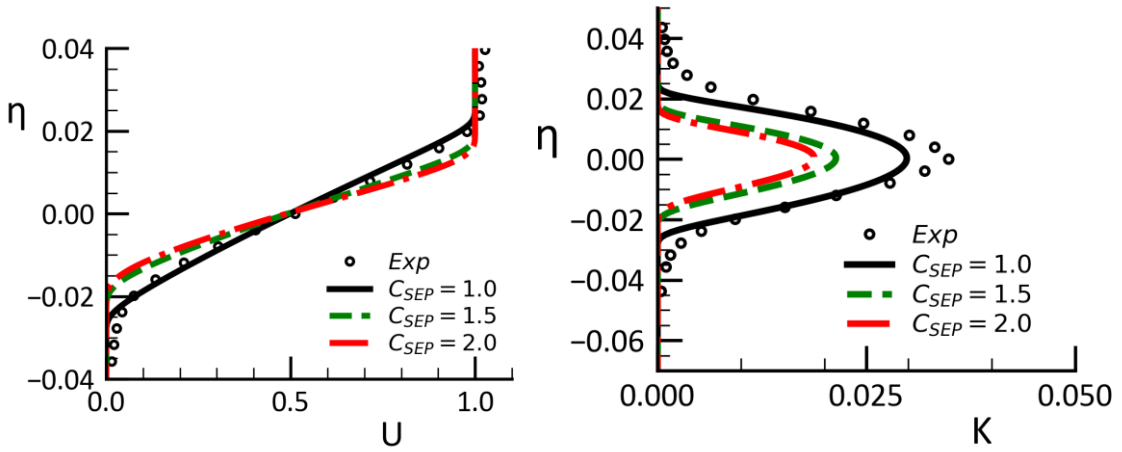

Figure 22: Impact of variation in C_{SEP} on mixing layer (C_{MIX}=0, C_{JET}=0.9, C_{NW}=0.5). Left: Velocity profile. Right: Turbulence kinetic energy profiles

In order to compensate the effect of C_{SEP} on free shear flows, the coefficient C_{MIX} has to be increased with increasing C_{SEP}. This is achieved by the correlation C_{MixCor} given in Equation (2.11) which is the model default. The correlation is provided so that users know which value is optimal for a given C_{SEP} setting. Increasing C_{MIX} above this value will lead to higher and decreasing it to lower turbulence levels and spreading rates for free shear flows.

The results for mixing layer simulations with $C_{MIX=}$ C_{MixCor} are shown in Figure 23. For all selected values of C_{SEP}, the mixing layer is maintained, and correct spreading rates are achieved.

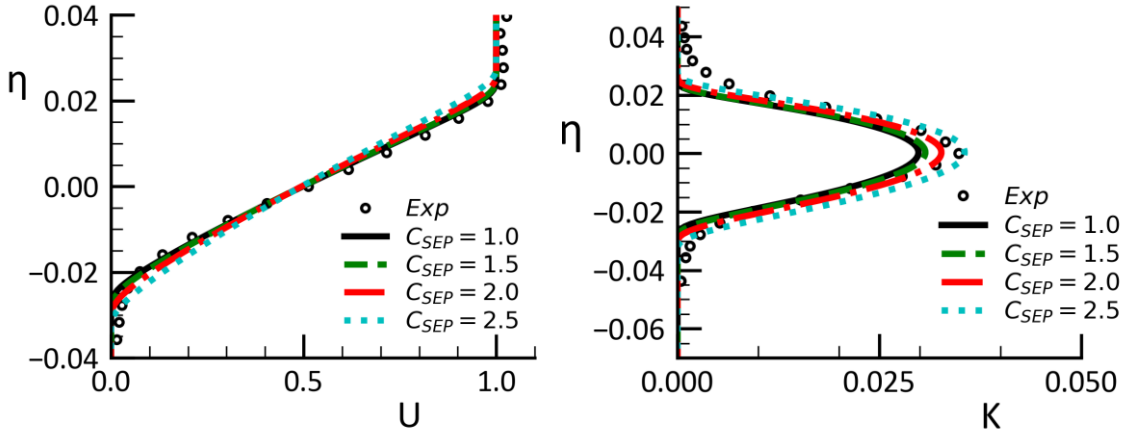

Figure 23: Impact of variation in C_{SEP} on mixing layer when using the C_{MIX}=$C_{MixCcor}$ correlation (C_{JET}=0.9, C_{NW}=0.5). Left: Velocity profile. Right: Turbulence kinetic energy profiles

3.4 The 'Jet' Parameter C_{JET}

The impact of the C_{JET} parameter is subtle and in most applications it can be maintained at its default value. It is important in cases where jet flows need to be computed with high accuracy. Remember that conventional models like k-ε or SST will over-predict spreading rates of round jets substantially while giving reasonable results for plane jets. For this so-called round-jet plane-jet 'anomaly' see e.g. [19,33].

The GEKO model is designed to provide parameter settings which allow an accurate representation of jet flow. This is achieved through the parameter C_{JET}. The way this is achieved is by reducing the influence of C_{MIX} (which increases mixing layer spreading rates) on jet flows (especially round jets). It should also be noted that the coefficient C_{JET} is a sub-function of the coefficient C_{MIX}. In case C_{MIX}=0, the coefficient C_{JET} has no impact.

Simulations are again based on self-similar jet-flow equations as given by Wilcox [33]. The two test cases are Wygnanski and Fielder [36] for the plane jet and Bradbury [4] for the round jet. Figure 24 shows simulations with C_{SEP}=2, C_{MIX}=0.35 (Correlation) and C_{NW}=0.5 (default). It is clearly seen that the model overpredicts the spreading rates especially for the round jet with C_{JET}=0. The effect of C_{JET} is to reduce the spreading rate of both jet flows, with C_{JET}=0.9 being close to both experimental data-sets. With C_{SEP}=2 and C_{JET}=0.9, the model avoids the round jet/plane jet anomaly and predicts lower spreading rates for the round than for the plane jet. Note again, that the changes of C_{JET} discussed here do not affect the mixing layer.

In contrast, Figure 25 shows a comparison between GEKO-1 (C_{SEP}=1.0) and GEKO-2 (C_{SEP}=1.0) with C_{JET}=0.9. As GEKO-1 is a close cousin of the standard k-ε model it behaves just like that model. It gives a correct spreading rate for the plane jet but over-predicts the round jet. Note again, that changes to C_{JET} in GEKO-1 would have no effect, as for that model C_{MIX}=0 (so that the sub-model C_{JET} is de-activated).

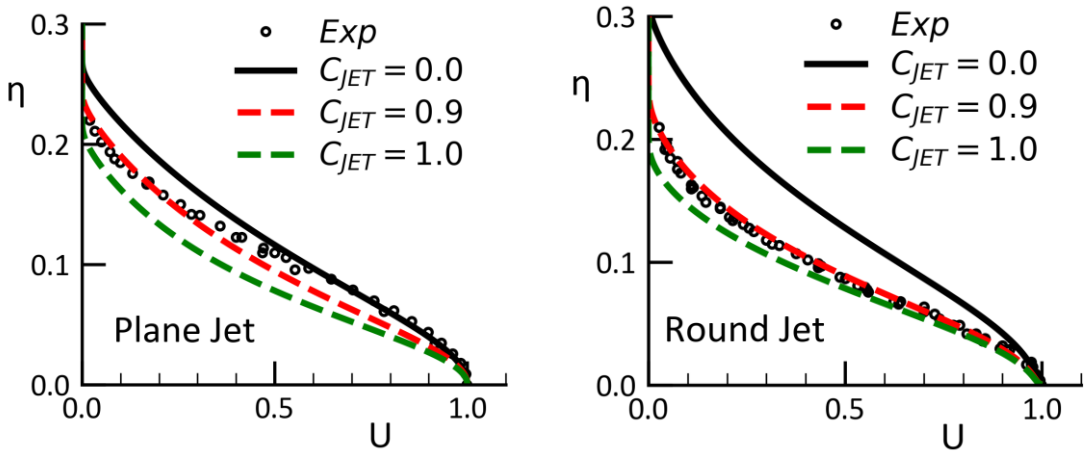

Figure 24: Effect of C_{JET} for plane (left) and round (right) jet flow (C_{SEP}=2.0, C_{MIX}=0.35, C_{NW}=0.5)

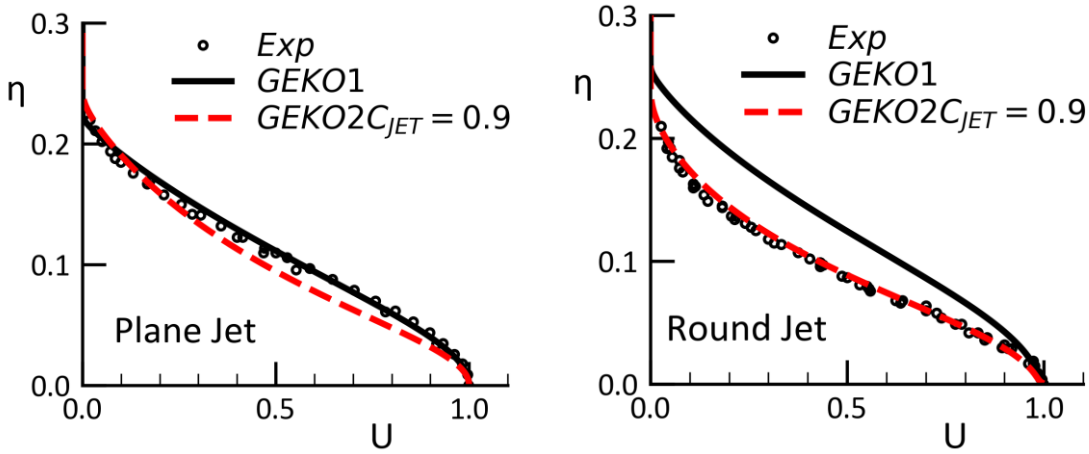

Figure 25: Comparison of GEKO-1 and GEKO-2 model (with variation of C_{JET}=0.9)

In summary, in order to achieve optimal performance for round jets, one needs to set C_{SEP} to values C_{SEP}~1.75-2.00 and C_{JET}=0.9 (default). With reduction in C_{SEP} and the corresponding reduction in C_{MIX}, the effect of C_{JET} vanishes.

There is another parameter CJET_AUX which also has an influence on the jet flow. It defines the limit between mixing layers and jet flows. The larger the value, the sharper the 'demarcation' and stronger the effect of C_{JET}. The default value is CJET_AUX =2.0. It is suitable for jet flow simulations to set the value to CJET_AUX =4.0. This is not done by default, as it can lead to oscillations on poor meshes.

Users who do not have a need for accurate predictions of jets can use the default settings for C_{JET}.

3.5 The 'Corner' Parameter C_{CORNER}

It is well known that for rectangular turbulent channel flows, secondary flows develop in the plane normal to the mean flow. Such secondary flow is not present in laminar flows and can also not be represented at all by eddy-viscosity models. The situation is depicted in Figure 26 for a square channel. The main flow direction is normal to the plotting plane. The velocity

contour colors on the left picture show the main flow as computed by a linear eddy-viscosity model. There are no streamlines when projected into this plane.

The practical effect of this effect is that the secondary flow transports flow (and thereby momentum) into the corner. If the corner flow experiences an adverse pressure gradient, this additional momentum can help the flow to avoid/delay separation. When computing such flows with an eddy-viscosity model, such separations can occur earlier than in the experiments, which in turn can have a substantial effect on the overall performance. The right picture shows the results from a Direct Numerical Simulation (DNS, e.g. [19]) of this flow. There are clearly recognizable secondary streamlines pushing flow into the corners. The center picture shows the GEKO model in combination with an existing non-linear algebraic stress-strain model (Wallin-Johansson Explicit Reynolds Stress Models WJ-EARSM), which can mimic the effect. The WJ-EARSM is fairly complex and the GEKO model was used as a reference point for calibration of the much simpler quadratic stress-strain relationship which can also account for this effect (Equation (2.7)). This term has a free parameter, C_{CORNER}, which can be tuned by the users.

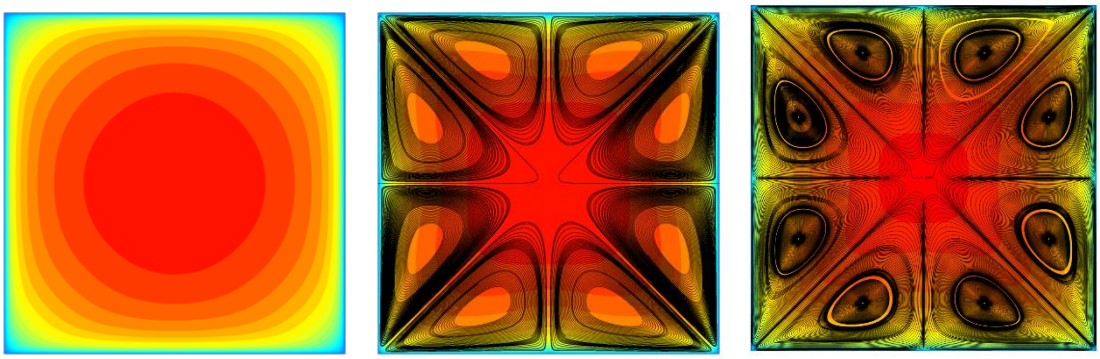

Figure 26: Comparison of streamline velocity contours and secondary motion predicted by linear (Left) and non-linear (Center) GEKO-1.00 model with the DNS (Right) data in the fully developed square duct flow [19]

Figure 27 shows a comparison for the rectangular channel for GEKO-175 (C_{SEP}=1.75 all else default). The left picture shows the combination of GEKO with the WJ-EARSM, the middle picture the combination with the quadratic term and C_{CORNER}=0.9 and the left for C_{CORNER}=0.0. The simple quadratic model gives a good approximation of the flow, similar to the WJ-EARSM.

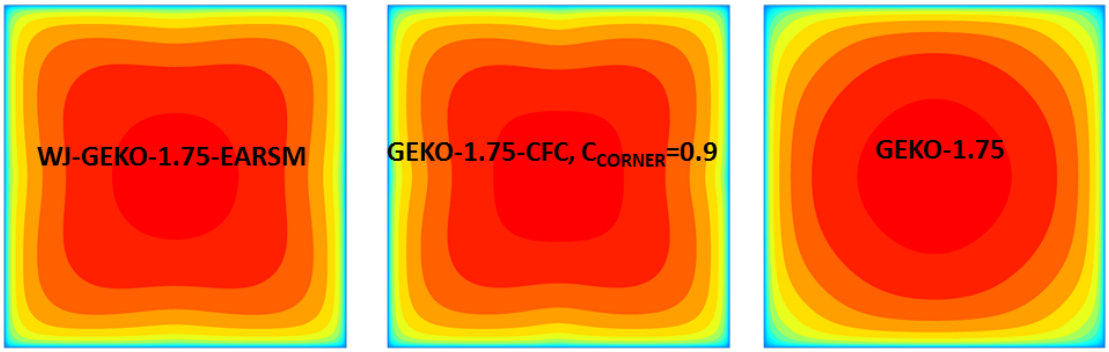

Figure 27: Comparison of turbulence models for flow in square channel. Left: GEKO with WJ-EARSM. Middle, GEKO with C_{CORNER}=0.9. Right GEKO linear (C_{CORNER}=0.0).

Figure 28 shows a comparison of velocity profiles for different turbulence models for the square channel. The right part of the picture shows the secondary flow into the corner along a diagonal of the channel cross-section. Most obviously, the linear model (GEKO-1.75) gives zero velocity along the diagonal. The other models provide fairly similar strength and distributions of the same order as the reference DNS data, but clearly also not in perfect agreement, especially very close to the wall. Note that further increases in C_{CORNER} for this flow would break the symmetry of the crossflow pattern. The left part of the figure shows the mean flow profile also along the diagonal. The most important effect is the higher velocity close to the wall ('fuller profile') which allows the flow to overcome a stronger pressure gradient before separating.

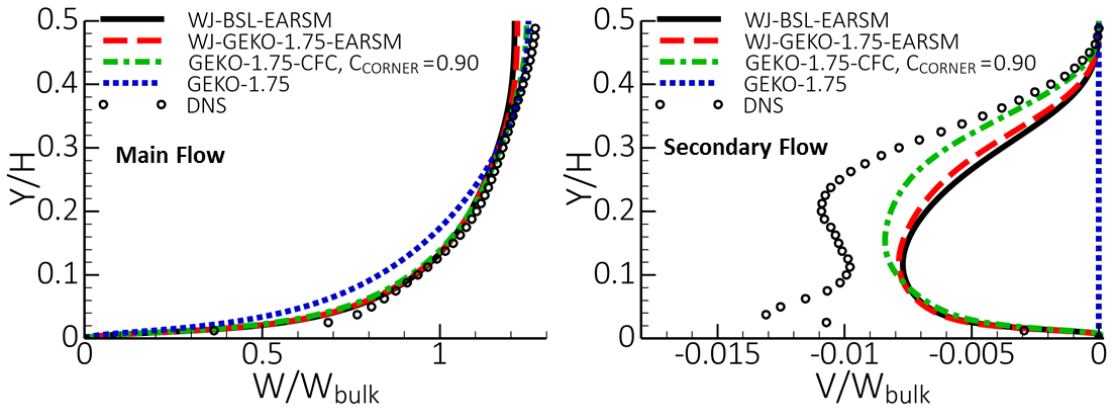

Figure 28: Velocity profiles plotted along diagonal of channel for different turbulence models against DNS data. Right: Main Flow, Left Secondary Flow.

A more challenging example is the flow in a 3D diffuser [5] shown in Figure 29. The diffuser has two opening angles, a large one on the upper wall and a small one at the side walls. In the experiments, the flow separates from one of the corners and then attaches to the lower wall. In the simulations, the flow topology depends strongly on the model and the corner flow representation.

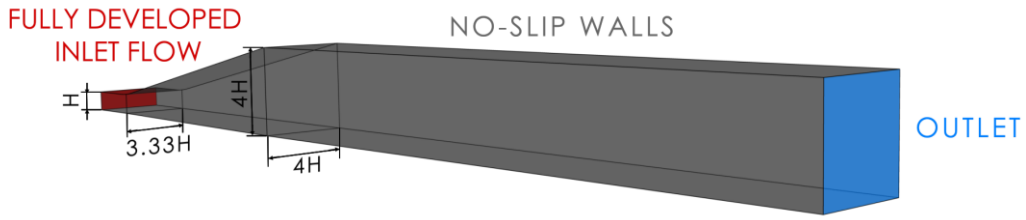

Figure 29: Geometry of 3D diffuser flow [4]

Figure 30 shows the mean velocity contours at the end of the expansion section of the diffuser. Clearly the flow topology depends strongly on the selected values of the corner flow correction term.

The influence of the model changes on the pressure coefficient, C_p, can be seen in Figure 31. Note that the current flow is very sensitive and hard to compute, but it does demonstrate the importance of corner flow separation for technical flows.

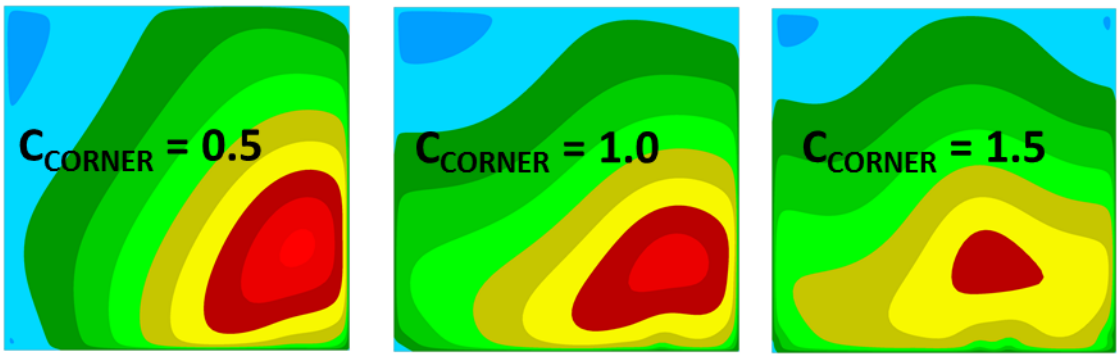

Figure 30: Flow topology for 3D diffuser flow shown through streamwise velocity contour at downstream end of diffuser opening section for GEKO-1.00 with different C_{CORNER} values.

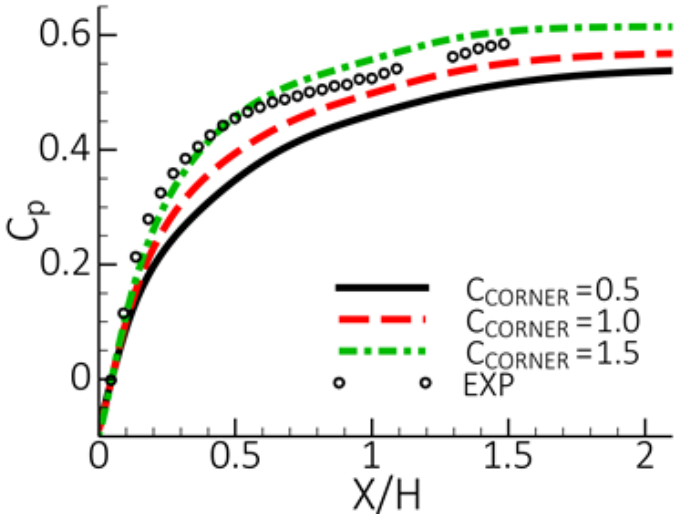

Figure 31: Wall pressure coefficient, C_p, for 3D diffuser for GEKO-1.00 with different C_{CORNER} values.

3.6 The 'Curvature' Parameter C_{CURV}

The curvature correction (CC) is an already existing model, which is accessible to all eddy-viscosity models in Fluent. The only change when integrating it with GEKO was that the coefficient C_{CURV} is now also accessible through a User Defined Function (UDF) and can thus be optimized zonally, or even locally.

No detailed description of the CC formulation is given, as it is described elsewhere [22]. The effect of the CC can be shown for a hydro-cyclone (see Figure 32) The flow (typically with particles) enters the domain tangentially through the feed. A strong swirl is generated pushing the particles to the wall and out through the underflow, whereas the cleaned fluid leaves the domain through the overflow. The effect of swirl and rotation cannot be handled by eddy-viscosity models without corrections. The current CC serves this purpose, as can be

seen by a comparison of the circumferential velocity profiles for the SST model, the SST-CC and a full Reynolds Stress model (RSM-SSG) in Figure 32. While the model without CC produces mostly a solid-body rotation, the SST-CC model gives results much closer to the experiments and similar to a full Reynolds Stress model (note that at the time of writing, the GEKO model has not been run for this test case. However, the effect of the CC is mostly independent of the underlying model formulation).

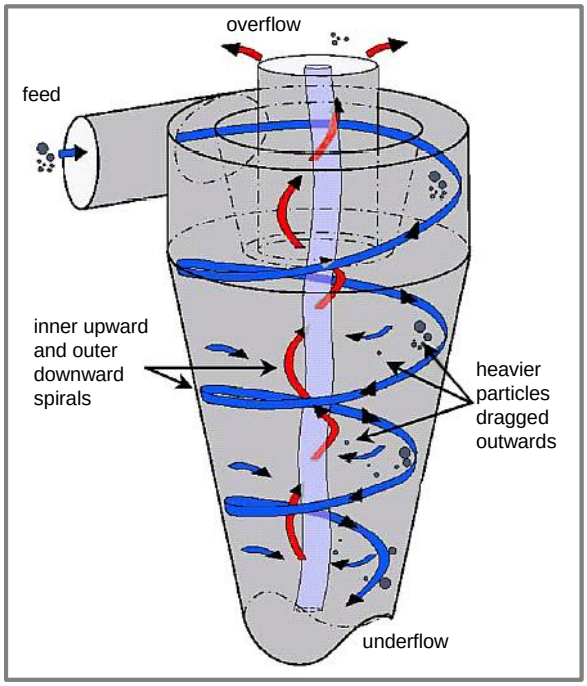

Figure 32: Hydrocyclone typical flow structure. Reproduced from Cullivan et al [9].

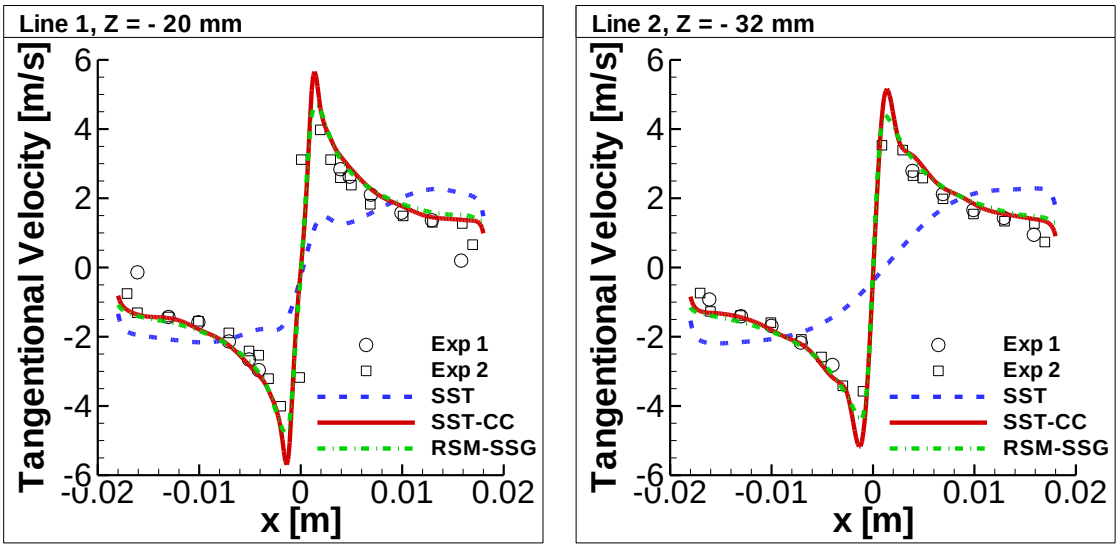

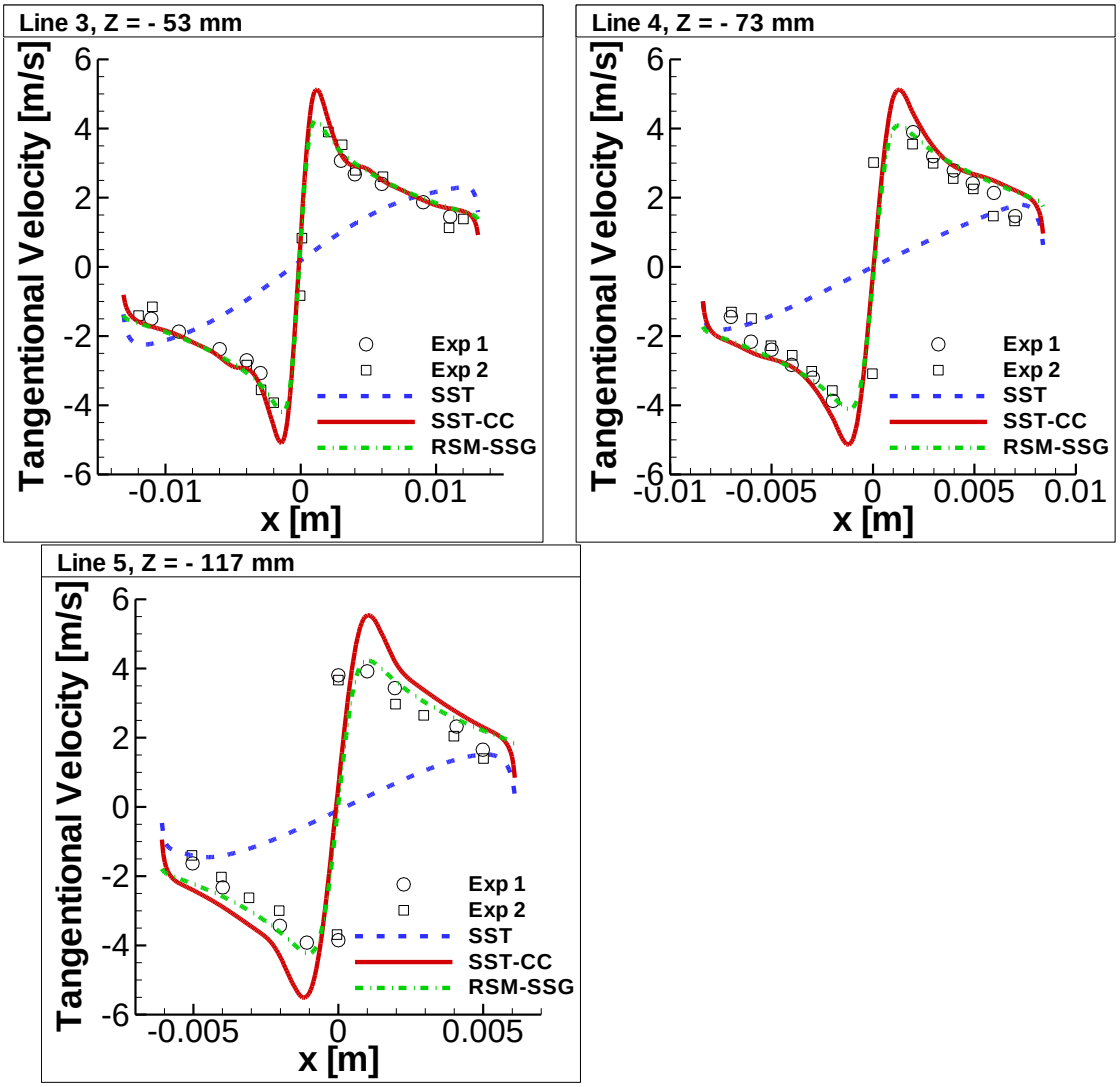

Figure 33: Time-averaged profiles of the tangentional velocity in the hydrocyclone. Comparison with the experiments of Hartley [13].

3.7 The Blending Function

The blending function activates the coefficients C_{MIX}/C_{JET}. In order to avoid any impact on boundary layers, the blending function is designed such that these parameters have only a minor effect there. In most cases the users will not have to change the function F_{GEKO} (in Fluent it is called 'Blending Function for GEKO'). However, there are several ways to modify the function in case it is needed.

The easiest way is to adjust the coefficients exposed in the GUI. For fully turbulent flows (no transition model) there is only one coefficient called CBF_TURB (GEKO). Increasing it will increase the thickness of the near wall 'shielding' and decreasing it will decrease the 'shielding' from C_{MIX}/C_{JET} inside the boundary layer. This effect can be seen in Figure 34 for the flow around a NACA 4412 airfoil. The lefts side of the figure shows the default setting (CBF_TURB=2) and the right side the function for CBF_TURB=4. The thickness of the boundary layer 'shielding' is clearly increased on the right part of the figure.

There is a second coefficient for this function, which is a bit more involved. It is introduced to allow protection of the laminar boundary layer from the C_{MIX}/C_{JET} term. This is desirable in case of transition predictions [16], where otherwise the C_{MIX}/C_{JET} term can affect the transition location. For this purpose, a second coefficient, CBF_LAM (GEKO) is used in case a transition model is selected. The effect is shown in Figure 35. The left figure shows the turbulent default (CBF_TURB=2.0, CBF_LAM=1.0 same as Figure 34 Left) and the right part shows the increase to its default for transitional simulations (CBF_TURB=2.0 CBF_LAM=25.0). As can be seen from the right part of Figure 34, the coefficient CBF_LAM provides increased shielding, especially in the leading edge region. In case of fully turbulent settings (no transition model), users can only access CBF_TURB (CBF_LAM=1.0 is fixed by default). The parameter CBF_LAM becomes available once a transition model is selected. The coefficient CBF_LAM needs to always satisfy $CBF\_LAM \geq 1$.

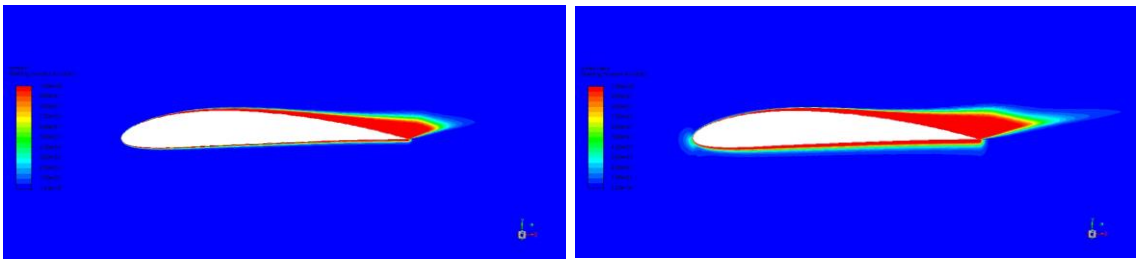

Figure 34: Effect of CBF_TURB on F_{GEKO} for flow around airfoil. Left CBF_TURB=2.0. Right: CBF_TURB=4.0.

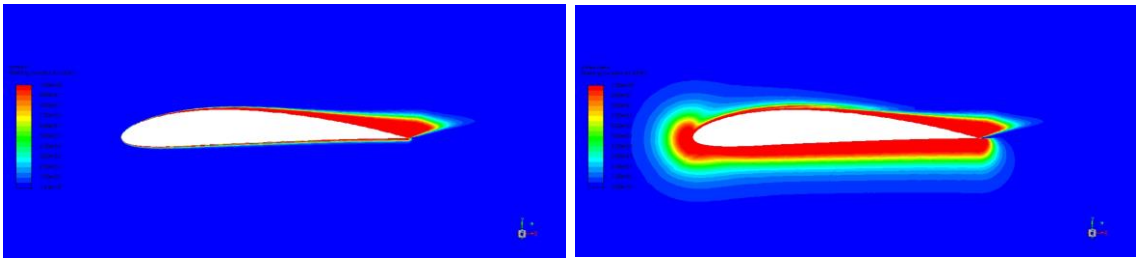

Figure 35: Effect of CBF_LAM on F_{GEKO} for flow around airfoil. Left CBF_LAM=1.0 (default for turbulent simulations). Right: CBF_LAM=25 (default for transitional simulations).

Finally, the function F_{GEKO} can be adjusted through a User Defined Function (UDF). Users can either over-write the function in the entire domain, or only in certain parts, as the original function is accessible in the UDF. This could make sense in areas where free shear flows and boundary layers cannot be easily discerned by the function itself, especially when C_{MIX} is increased to obtain more mixing in the free shear flow region.

An example of such a flow is shown in Figure 36 for a multi-element airfoil. Assume, the wake of the slat (upstream airfoil) over the main airfoil is of interest. Assume that the default settings provide not enough mixing in this region, hence an increased mixing through increases in C_{MIX} is desired. This works for moderate increases in C_{MIX}, but large increases (like C_{MIX}=3) lead to decreasing efficiency of the C_{MIX} term. The reason is that through increases in the eddy-viscosity, the blending function becomes activated also in the wake, due to the proximity of the main airfoil wall. This is shown in the middle part of Figure 36, where one can clearly see the activation of the blending function in the wake of the slat. To counter such an effect, one can over-write the blending function. In the current case, a function based

on wall-distance was used as shown in the right part of Figure 36. Note that this is just a generic example to demonstrate the issues and no effort was made to optimize the bending function. The effect of the change in the function F_{GEKO} is seen in Figure 37 which shows the ratio of turbulence to molecular viscosity for the blending functions and settings shown in Figure 36. Clearly, the ratio increase from the left (default settings) to the middle picture. However, the increase is moderate. When restricting the function F_{GEKO} to the immediate boundary layer around the main wing, the effect of increasing C_{MIX} becomes much stronger, resulting in a substantial increase in the viscosity ratio (Figure 37 – right).

It needs to be stressed again, that such modifications of F_{GEKO} are typically not required and the flexibility of provided by simply changing coefficients is sufficient in most cases. However, the discussion shows the versatility of the current GEKO models implementation.

.

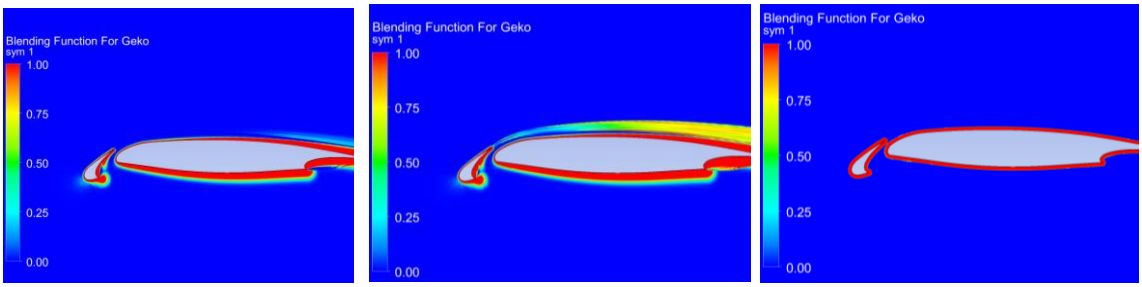

Figure 36: Blending function F_{GEKO} for multi-element airfoil. Left: Default C_{SEP}=1.75, C_{MIX}=C_{MixCor}=0.303. Middle: C_{MIX}=3. Right: F_{GEKO} through UDF

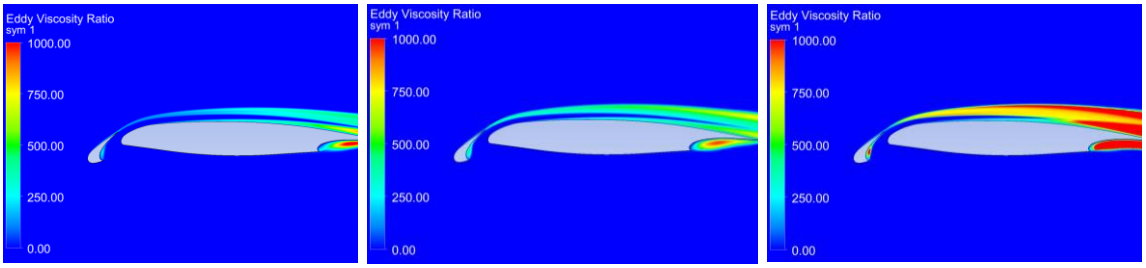

Figure 37: Ratio of turbulence to molecular viscosity for multi-element airfoil. Left: Default C_{SEP}=1.75, C_{MIX}=C_{MixCor}=0.303. Middle: C_{MIX}=3. Right: F_{GEKO} through UDF

A more dramatic example of how the change in blending function can affect results is given by the flow around a triangular cylinder. The set-up is shown in Figure 38.

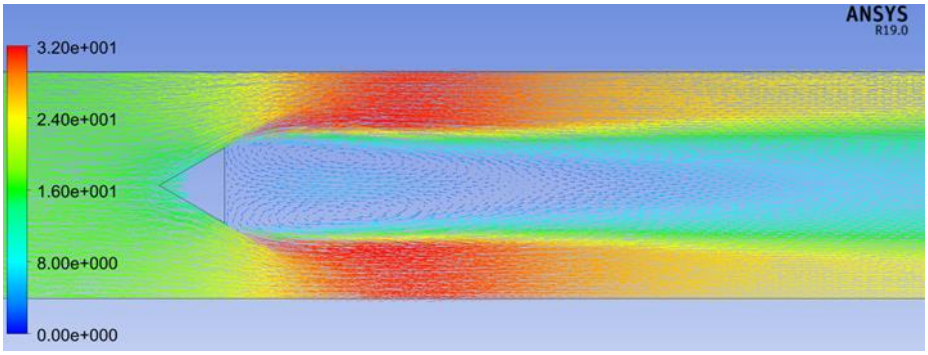

Figure 38: Flow around triangular cylinder [37]

The cylinder has an edge length of $L = 0.04m$, the height of the channel is $H = 0.12m$. The inlet velocity is $U{\sim}16\ m/s$. The simulation is carried out in steady state mode – and converges to a steady state solution (which is not always possible with bluff body flows). The real flow is of course unsteady with strong vortex shedding in addition to turbulence created unsteadiness. The vector field depicted shows a very large separation zone downstream of the cylinder, as expected. The simulation was carried out with GEKO-1.75 (default) under steady-state conditions.

In order to test by how much, the re-circulation zone can be reduced, the C_{MIX} coefficient was increased. The results are shown in Figure 39 when using the built-in version of the F_{GEKO} function. The recirculation (line in middle figure) decreases with increasing C_{MIX}. However, eventually, the entire separation zone lies within the F_{GEKO}=1 region and no further effect can be achieved by increasing C_{MIX}.

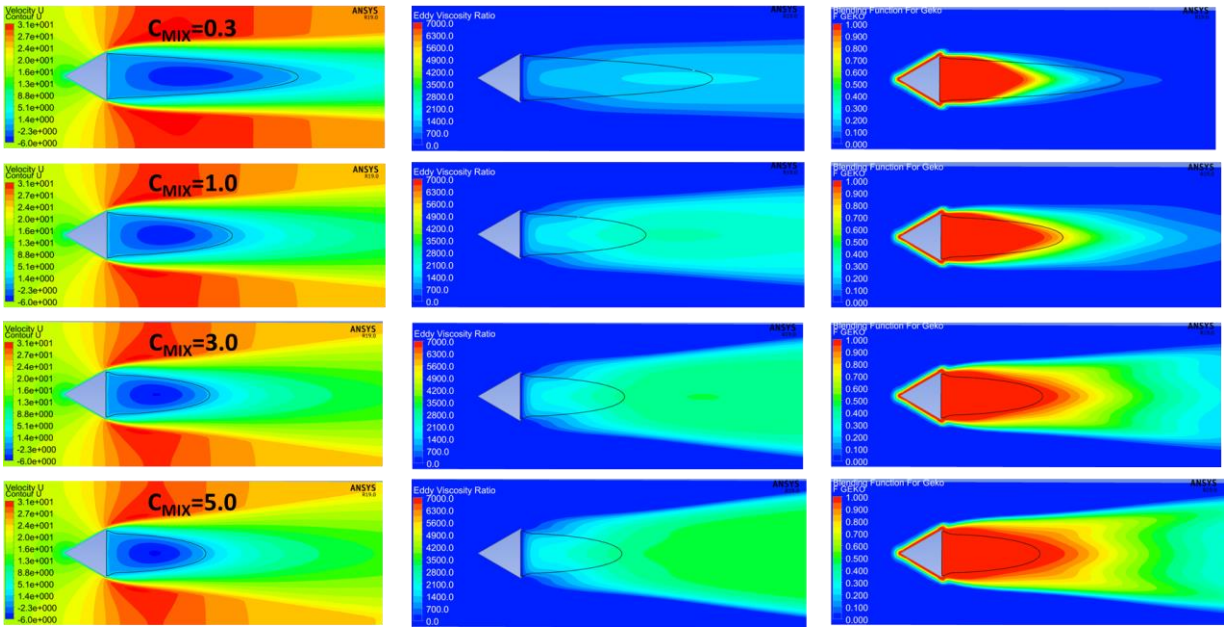

Figure 39: GEKO-1.75 solution under variation of C_{MIX}. Left: Velocity U. Middle: Eddy-viscosity ratio. Right: F_{GEKO} using built-in function [28]

The same tests are shown in Figure 40 but with the help of a UDF-based F_{GEKO} function. As shown in the right part of the figure, F_{GEKO} is defined only within a given wall distance as F_{GEKO}=1 and is switched to free shear flow status outside. This avoids the restriction of the impact of increasing CMIX and allows a further reduction in the re-circulation zone due to increased mixing.

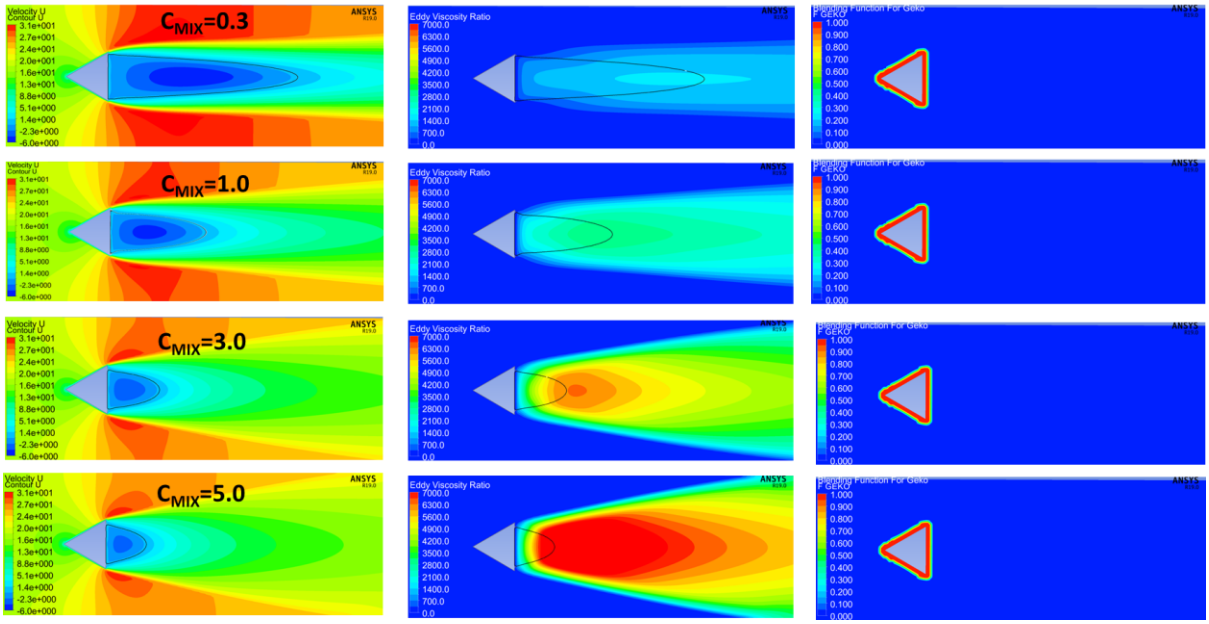

Figure 40: GEKO-1.75 solution under variation of C_{MIX}. Left: Velocity U Middle: Eddy-viscosity ratio. Right: F_{GEKO} using UDF-based function [28]

The comparison with experimental data along the center-line downstream of the cylinder is shown for both F_{GEKO} variants in Figure 41. The left part of the figure shows the solution using the built-in function for F_{GEKO} and the right part shows the solution using a wall-distance-based UDF variant (as shown in right part of Figure 40). Clearly, the UDF based variant allows a much stronger reduction in separation size. It should be noted that none of the simulations is able to produce the fairly strong backflow velocity in the re-circulation zone. This should not come as a surprise, as it is mostly a result of very strong backflow events in the unsteady vortex shedding cycle of the experiment, which cannot be captured by a steady state solution. Nevertheless, it is important to observe the much better agreement in flow recovery downstream of the recirculation zone. In case of more complex arrangements, any additional parts of the geometry downstream of the triangular cylinder would see a much more realistic approaching flow field than with the default settings.

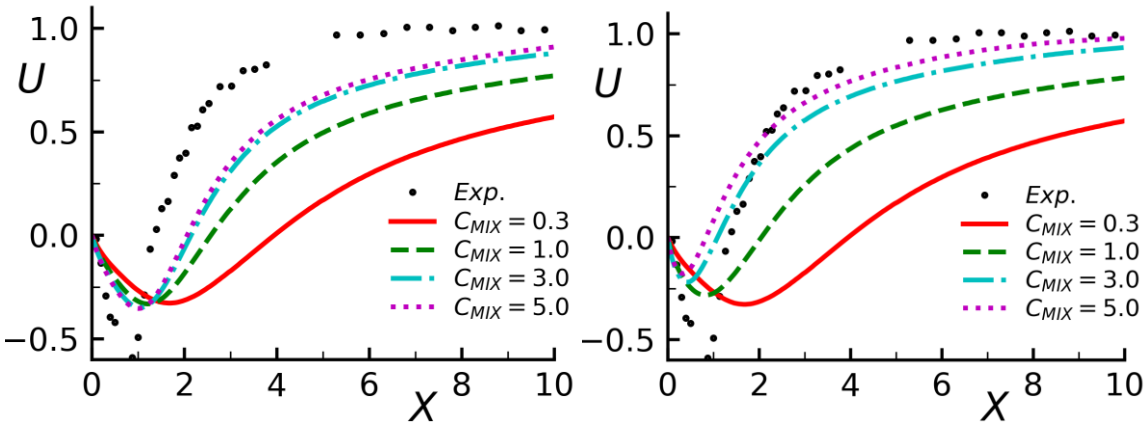

Figure 41: Center line velocity for triangular cylinder. Left: GEKO-1.75 with built-in F_{GEKO} function. Right: GEKO-1.75 with UDF-based F_{GEKO} function [28]

3.8 Other Special Coefficients

The realizability coefficient is set to its standard value of C_{REAL}=0.577. The value should typically not be changed but is accessible for special situations. However, it was found that limiters can have a strong effect for flows which are severely under-resolved. An example would be an inlet condition for the velocity field, where the velocity in the lower half of the inlet has one value and in the upper half another. At the jump between these two values, the flow is under-resolved and the coefficient C_{REAL} could potentially delay the growth of the mixing layer. Note that for such flows, the production limiter could have a similar effect. If this is the case, it would be an option to set both limiters to very large values and instead activate the Kato-Launder limiter.

The coefficient CNW_SUB allows for slight re-tuning of the log-layer shift which will also affect the wall shear stress distribution for boundary layers. Increasing its value from CNW_SUB=1.7 will shift the log-layer more into the laminar direction (up) and decrease the wall shear stress.

4 Strategies for Model Optimization

Most users are intimidated/scared of the prospect to modify turbulence model coefficients. Part of the reason for this lies in the interconnectedness of coefficients in conventional turbulence models, where any change to any coefficient can have detrimental effects even on the simplest flows, like flat plate boundary layers (which users typically do not want to modify). Still, a conservative attitude is also commendable for the GEKO model, even though the effects of coefficient changes are much more predictable. The model should therefore only be adjusted if other sources of error have been minimized (it is not always the turbulence model's fault if things do not match). In addition, modifications should be guided by experimental data as far as possible.

4.1 GEKO Defaults

The defaults for the GEKO model have been selected to match the SST models performance as closely as possible for the building block flows. Especially for boundary

layers, the defaults predict very close results to those of the SST model. The SST model is used in many industrial CFD simulations already, so the default selected for the GEKO model provides a fairly save conversion from SST to GEKO.

There is another 'fix point' in coefficient settings. With the combination C_{SEP}=1.0, C_{NW}=1.0, which automatically sets C_{MIX}=0.0 from the correlation C_{MixCor} (note again that C_{MIX}=0.0 renders C_{JET} passive, as it is a sub-model to C_{MIX}). This setting is an exact transformation of the standard k-ε model (except for the wall treatment and the realizability limiter). Users who have used the k-ε model successfully in the past, are therefore advised to use these settings.

Figure 42 shows a comparison of GEKO model settings for the NACA 4412 airfoil [32] against their 'reference' model. Two model pairs are clearly visible (GEKO-1, RKE) and (GEKO-175, SST) – each pair giving almost identical results.

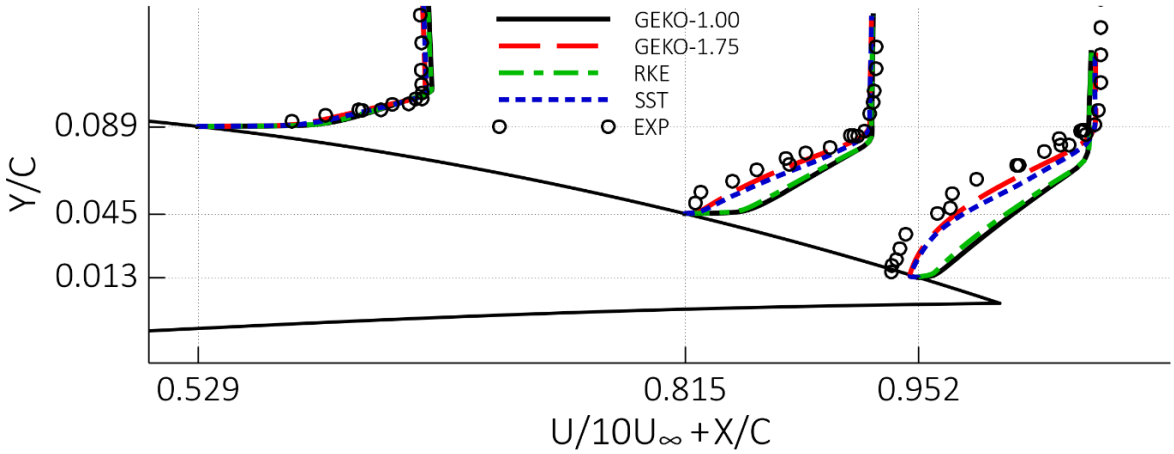

Figure 42: Comparison of velocity profiles for flow around the NACA-4412 airfoil [32]

4.2 Optimizing Coefficients

C_{SEP}

The most important coefficients for most applications is C_{SEP}. It controls the separation points/lines from smooth body-separation. In case the flow is dominated by boundary layers, users should only modify this coefficient and explore if values within the range given by Equation (2.10) are sufficient for obtaining improved results. Again, increasing C_{SEP} will lead to stronger/earlier separation. When changing C_{SEP} one should in a first step keep all other coefficients at their default values.

C_{NW}

The coefficient C_{NW} should only be changed if detailed near wall or surface information needs to be matched and if this cannot be achieved by optimizing C_{SEP} alone. The most prominent example would be optimizations with respect to heat transfer coefficients or oil-flow pictures from experiments. Increasing C_{NW} will increase heat transfer and wall shear stress levels in non-equilibrium regions.

C_{MIX}

In some cases, standard settings (or models) under-estimate the turbulent mixing in free shear flows. The coefficients C_{MIX} will allow an adjustment under such scenarios. Increasing C_{MIX} will increase eddy-viscosity levels in such zones. It should be noted that this is only possible within physical limits. E.g. in some cases, strong mixing is observed behind bluff bodies. Such effects often result from vortex shedding and cannot be covered fully by a steady state turbulence model run. However, increasing C_{MIX}, can improve such situations relative to default settings (see Figure 40). In case changes to C_{MIX} do not show the desired influence, it is advisable to check the blending function F_{GEKO}. It should be recalled that C_{MIX} is only effective in regions where $F_{GEKO} \neq 1$. In case, C_{MIX} is de-activated by F_{GEKO} in the region of interest, modifications to the F_{GEKO} function might be required.

C_{JET}

The coefficient C_{JET} is subtle. As the name implies it should only be considered when jets are present in the domain. Regions with round jets should best be computed with $C_{SEP} = 1.75 - 2.00$ as otherwise the effect of C_{JET} is not strong enough to achieve the desired effect. In case these settings for C_{JET} are not suitable in the entire domain, one can set these values also locally through UDF access. For highly accurate jet simulations also set CJET_AUX =4.0 (it activates the C_{JET} function more aggressively).

In summary – for the free shear flows, the GEKO-1 model behaves like the underlying *k-*ε model, with good spreading rates for the mixing layer and plane jet but an over-prediction of spreading for the round jet. When increasing C_{SEP} one also needs to adjust C_{MIX} to maintain proper spreading for the mixing layer. This is automatically achieved through a correlation relating these two coefficients (C_{MIX}=C_{MixCor}). To avoid over-prediction of spreading rates for jets, with increasing C_{MIX}, the coefficient C_{JET} is introduced. A value of C_{SEP}=2 and C_{JET}=0.9 provides correct asymptotic spreading for both, the round and the plane jet. In case stronger mixing is required, the coefficient C_{MIX} can be increased relative to its correlation value. In some cases, it might even be desirable to modify the blending function F_{GEKO} to obtain an even stronger effect for mixing layers near walls (see 3.7).

C_{CORNER}, C_{CURV}

The coefficients C_{CORNER} and C_{CURV} are also available for other k-ω models. They can be activated in combination with GEKO as required by the simulation.

Wall Distance Free

The GEKO model can also be run without a need for computing the wall distance. This is desirable for cases with moving grids/geometries. If the 'wall-distance-free' option is selected the coefficients C_{MIX}/C_{JET} are de-activated. In order to still achieve proper mixing layer growth, set C_{SEP}=1.

5 Summary

A new RANS concept has been introduced. The new model is termed Generalize *k-*ω model (GEKO). It is based on a *k-*ω model platform and is designed to consolidate RANS turbulence models in ANSYS CFD. Instead of offering a wide range of different models, it is the goal to provide a single model, with the flexibility to adjust it to a wide range of generic flow conditions and applications.

Flexibility within GEKO is achieved by augmenting the model with free coefficients, which can be adjusted by the user without the danger of violating the basic model calibration for conventional free shear flows and boundary layers. This allows the user to tune the model in a safe parameter space without the need for expert knowledge in turbulence modeling. In other words, instead of switching between a large number of existing turbulence model to find the optimal one for a given application, the user can now stay within one model framework and simple adjust the free coefficients. The model is designed such that the modification of the coefficients allows coverage of a wide solution space (actually a wider space than by switching between existing models).

In addition to being able to adjust the model coefficients, GEKO offers the advantage that the variation of coefficients is much more transparent than the change between different models. By changing from one model to another (say from SST to k-ε) one does not only switch the model but also numerous other settings (e.g. different limiters, different wall treatment, …). Such changes might have an additional large effect on the solution without being transparent to the user. Finally, not all options/extensions are compatible with all turbulence models. Case in point is that models for laminar-turbulent transition are not compatible with existing k-ε models. A k-ε model user who wants to add transition physics, will therefore need to first switch to a k-ω model and then activate the transition model. It will then be difficult to attribute solutions changes to any one of the two changes made in the settings. Within GEKO, the user can make changes step by step and observe their impact on the solution separately, as all options are (or will be made) available within this model framework.

It is to be emphasized that users do not have to adjust coefficients. There are strong default settings (similar to the SST model) and there are further recommendations for settings to mimic other existing models like k-ε. It is however assumed that many simulation results can significantly be improved by very few changes to the GEKO coefficients. For simple geometries, a global optimization of the coefficients is typically sufficient. For more complex application, where several different turbulence-related phenomena are included in one set-up, the coefficients can be set via UDFs zonally. In the longer run, it can also be anticipated that the free coefficients can be used for automatic optimization and Machine Learning.

6 Example UDFs

This UDF overwrites the blending function F_{GEKO} in regions where $x \leq 2$:

```
#include "udf.h"
DEFINE_KW_GEKO_BF(user_geko_bf, c, t)
 {
   real bf_value;
   real xc[ND_ND];
   C_CENTROID(xc,c,t);
   if (xc[0] > 2.0)
     bf_value = Get_Geko_Blending_Function (c, t,
              C_R(c,t), C_MU_L(c,t), C_WALL_DIST(c,t),
              C_K(c,t), C_O(c,t));
   else
     bf_value = 1.0;
```

```
  return bf_value;
}
```

7 References

1. Albertson, M.L., Dai Y.B., Iensen, R.A. and Rouse H. (1948): "Diffusion of submerged jets", Proc. of ASME, v.74.
2. Bachalo, W. D. and Johnson, D. A., (1986): "Transonic, Turbulent Boundary-Layer Separation Generated on an Axisymmetric Flow Model," AIAA Journal, Vol. 24, No. 3, , pp. 437-443.
3. Bell, J. H. and Mehta, R. D., (1990): "Development of a two-stream mixing layer from tripped and untripped boundary layers", AIAA J., vol. 28, no.12, pp. 2034-2042.
4. Bradbury, L.J.S., (1965): “The Structure of a Self-Preserving Plane Jet”, Journal of Fluid Mechanics Vol. 23, pp.31-64.
5. Buice, C.U. and Eaton, J.K., (2000): "Experimental Investigation of Flow Through an Asymmetric Plane Diffuser", Journal of Fluids Engineering, Vol. 122, pp. 433-435. 96.
6. Cebeci, T. and Bradshaw, P., (1988): “Physical and Computational Aspects of Convective Heat Transfer”, 1st ed. 1984/2nd ed. 1988, Springer-Verlag.
7. Coles, D.E., and Hirst, E.A., Eds, (1969): "Computation of turbulent boundary layers- 1968 AFOSR-IFP-Stanford Conference". Vol. 2, Stanford University, CA.
8. Cook, P.H., M.A. McDonald and M.C.P. Firmin, (1979): "Aerofoil RAE 2822 - Pressure Distributions, and Boundary Layer and Wake Measurements," Experimental Data Base for Computer Program Assessment, AGARD Report AR 138,
9. Cullivan, J.C. Williams. R.A., Dyakowski T. and Cross C.R., (2004): “New understanding of a hydrocyclone flow field and separation mechanism from computational fluid dynamics”. Minerals Engineering, Vol.17 No.5, 2004.
10. Driver, D.M., (1991): "Reynolds Shear Stress Measurements in a Separated Boundary Layer Flow", AIAA 22nd Fluid Dynamics, Plasma Dynamics and Laser Conference, AIAA-91-1787.
11. Durbin, P.A. and Reif, B.A., (2001): “Statistical Theory and Modeling for Turbulent Flows,” John Wiley & Sons.
12. Durbin, P.A. (1991): "Near-wall turbulence closure modeling without ‘damping functions’". Theor. Comput. Fluid Dyn. 3(1).
13. Hartley, C.D., (1994): “Measurement of flow velocities within a hydrocyclone using laser doppler anemometry”, Technical Report FTN/X/82, AEA, Power Fluidics, BNFL
14. Jones W. P. and Launder B. E. (1972): “The Prediction of Laminarization with a Two-Equation Model of Turbulence. Int. J. Heat Mass Transfer., 15:301–314.

15. Kato, M., and Launder, B.E., (1993): "The modelling of turbulent flow around stationary and vibrating square cylinders". In Proc. Ninth Symposium on Turbulent Shear Flows, volume 9, page 10.4.1, Kyoto, Japan.
16. Langtry, R.B. and Menter, F.R. (2009): "Correlation-Based Transition Modeling for Unstructured Parallelized Computational Fluid Dynamics Codes". AIAA J. 47(12), 2984-2906.
17. Mani, M., Babcock, D. A., Winkler, C. M., and Spalart, P. R., (2014): "Predictions of a Supersonic Turbulent Flow in a Square Duct," AIAA Paper 2013-0860, January 2013.
18. Menter, F.R. (1994): "Two-equation eddy-viscosity turbulence models for engineering applications", AIAA Journal, Vol. 32, No. 8, pp. 1598-1605.
19. Pope, S.B. (1978): "An explanation of the turbulent round-jet/plane-jet anomaly", AIAA Journal, Vol. 16, No. 3, pp. 279-281.
20. Raiesi, H., Piomelli and U., Pollard, A. (2011): "Evaluation of Turbulence Models Using Direct Numerical and Large-Eddy Simulation Data". Journal of Fluids Engineering, v.133, No.2, 021203 (10 pp.).
21. Skare, P. E., and Krogstad, P., (1994): "A Turbulent Equilibrium Boundary Layer Near Separation," J. Fluid Mech., 272, pp. 319–348.
22. Smirnov P. E. and Menter F. R., (2008): *"*Sensitization of the SST Turbulence Model to Rotation and Curvature by Applying the Spalart-Shur Correction Term*". ASME Paper GT 2008-50480*. Berlin, Germany.
23. Somers, D. M. (1997): "Design and Experimental Results for the S805 airfoil", NREL/SR-440-6917
24. Somers, D. M. (2005): "Design and Experimental Results for the S825 Airfoil", NREL/SR-500-36346
25. Somers, D. M. (1997): "Design and Experimental Results for the S809 Airfoil", NRELSR-440-6918.
26. Somers, D. M. (1997): "Design and Experirltental Results for the S814 airfoil", NREL/SR-440-6919.
27. Spalart P. R. and Shur M. L, (1997): *"*On the Sensitization of Turbulence Models to Rotation and Curvature*"*. Aerospace Sci. Tech. 1(5). 297–302.
28. Sjunnesson, A. Nelsons C. and Max E., (1991): *"*LDA measurement of velocities and turbulence in a bluff body stabilized flame*".* Volvo Flygmotor AB, Trollhattan
29. Timmer W. A. and van Rooij R. P. J. O. M. (2003): "Summary of the Delft University Wind Turbine Dedicated Airfoils", AIAA Paper, 2003-0352
30. Van der Hegge Zijnen B.G., (1959): "Measurement of turbulence in a plane jet of air by the diffusion method and by hot-wire method". Appl. Sci. Res., S.A., vol.7, No. 4.
31. Vogel, J.C. and Eaton, J.K., (1985): "Combined Heat Transfer and Fluid Dynamic Measurements Downstream of a Backward-Facing Step", Vol. 107, Journal of Heat Transfer, pp. 922 – 929.
32. Wadcock, A. J. (1987): "Investigation of Low-Speed Turbulent Separated Flow Around Airfoils", NASA Contractor Report 177450
33. Wilcox, D.C. (2006): *Turbulence Modeling for CFD,* DCW Industries Inc., 3rd. Edition.
34. Wilcox, D.C, (2007): "Formulation of the k-ω Turbulence Model Revisited", AIAA Paper 2007-1408.
35. Wolfshtein. M. (1969): "The Velocity and Temperature Distribution of One-Dimensional Flow with Turbulence Augmentation and Pressure Gradient". Int. J. Heat Mass Transfer. 12. 301–318.

36. Wygnanski, I. and Fiedler, H.E., (1968): “Some Measurements in the Self-Preserving Jet”, Boeing Scientific Research Labs, Document D1-82-0712.